Activation of Triruthenium Carbonyl Complexes by Incorporation of Hemilabile Ancillary Ligands Containing Alkoxo, Amido, or Thiolato Groups. Generation of a Reactive Alkenyl Complex

Noël Lugan, François Laurent, Guy Lavigne,* Timothy P. Newcomb, Eric W. Liimatta, and Jean-Jacques Bonnet

Laboratoire de Chimie de Coordination du CNRS, Associé à l'Université Paul Sabatier et à l'Institut National Polytechnique, 205, route de Narbonne, 31077 Toulouse Cedex, France

Received July 30, 1991

The alkoxo, amido, or thiolato groups derived respectively from 2-hydroxypyridine, 2-anilinopyridine, or 2-mercaptopyridine are incorporated into $Ru_3(CO)_{12}$ to give several "activated" anionic and neutral complexes. The anions $[Ru_3(\mu\text{-}\eta^2\text{-}X(C_5H_4N))(CO)_{10}]^-$ (**1a,c**) and $[Ru_3(\mu_3\text{-}\eta^2\text{-}X(C_5H_4N))(CO)_9]^-$ (**2a,b**): **a**, X = $N(C_6H_5)$; **b**, X = S; **c**, X = O) are obtained (i) in 80–90% yield by treatment of $Ru_3(CO)_{12}$ with $K[X(C_5H_4N)]$ followed by metathesis with (PPN)Cl (PPN = $(C_6H_5)_3PNP(C_6H_5)_3^+$) or (ii) by reaction of $HX(C_5H_4N)$ with $PPN[Ru_3(\mu\text{-}H)(CO)_{11}]$ (refluxing THF, 2 h, 60% yield). The amido derivatives **1a–3a** are also available via method iii, involving direct reaction of 2-anilinopyridine with $Ru_3(CO)_{12}$ (refluxing benzene, 2 h) to give $Ru_3(\mu\text{-}H)(\mu_3\text{-}\eta^2\text{-}N(C_6H_5)(C_5H_4N))(CO)_9$ (**3a**) (yield 85%). The latter is subsequently deprotonated by $PPNBH_4$ to give **2a** (yield 90%). The sulfido derivative $Ru_3(\mu\text{-}H)(\mu_3\text{-}\eta^2\text{-}S(C_5H_4N))(CO)_9$ (**3b**) is obtained in 80–90% yield by protonation of the potassium salt of **2b**. The X-ray structures of the PPN salts of **1c** and **2a** are reported. Crystallographic data for PPN·**1c**: triclinic $P\bar{1}$ (No. 2), a = 13.209 (1) Å, b = 18.149 (2) Å, c = 11.217 (2) Å, α = 102.37 (1)°, β = 96.52 (1)°, γ = 107.40 (1)°, V = 2461 Å^3, Z = 2; μ(Mo Kα) = 10.15 cm^{-1}; R = 0.042, R_w = 0.043 for 7330 observations and 382 variables. Crystallographic data for PPN·**2a**: triclinic $P\bar{1}$ (No. 2), a = 15.933 (2) Å, b = 17.163 (2) Å, c = 10.384 (2) Å, α = 102.69 (1)°, β = 91.06 (1)°, γ = 107.55 (1)°, V = 2630 Å^3, Z = 2; μ(Mo Kα) = 8.64 cm^{-1}; R = 0.042, R_w = 0.042 for 5665 observations and 364 variables. On the basis of these structures, it is suggested that the variable hapticity of group X (terminal position in **1** and bridging position in **2**) plays a "lightly stabilizing" role for coordination sites. The hydrido complexes $Ru_3(\mu\text{-}H)(\mu_3\text{-}\eta^2\text{-}X(C_5H_4N))(CO)_9$ (**3a,b**) react cleanly with alkynes (40–50 °C, 30–45 min) to give selectively the corresponding alkenyl complexes $Ru_3(\mu_3\text{-}\eta^2\text{-}X(C_5H_4N))(\mu\text{-}(C_6H_5)CCH(C_6H_5))(CO)_8$ (**4a**, 90–95% yield; **4b**, 70–80% yield) via cis insertion into the metal–hydride bond. The X-ray structure of **4a** has been determined. Crystallographic data for **4a** (crystallizing with 1 mol of CH_2Cl_2 per unit cell): triclinic $P\bar{1}$ (No. 2), a = 10.424 (1) Å, b = 18.795 (2) Å, c = 8.964 (1) Å, α = 93.97 (1)°, β = 105.09 (1)°, γ = 78.51 (1)°, V = 1661 (5) Å^3, Z = 2; μ(Mo Kα) = 13.76 cm^{-1}; R = 0.023, R_w = 0.025 for 5502 reflections and 436 variables. The cluster consists of a trinuclear ruthenium unit supported by a face-bridging phenylpyridylamido group. The bridging alkenyl group is coordinated at equatorial sites and spans a metal–metal edge adjacent to that supported by the bridging amido group. There is a bridging carbonyl spanning the same edge as the amido group. The features which may account for the high reactivity of this complex are discussed.

Introduction

There is growing evidence from the recent literature that a variety of nucleophilic anions including alkoxides,[1] amides,[2] halides,[3] and pseudo halides[4] are prone to enhance the activity of ruthenium carbonyl cluster complexes and thus bring selectivity in their reactions with organic substrates.[5,6]

In parallel to earlier observations that changes in attachment of halides or pseudo-halides provide a low activation energy path for coordination of substrates in some anion-promoted systems[3,4,6] (see eq 1), we were prompted

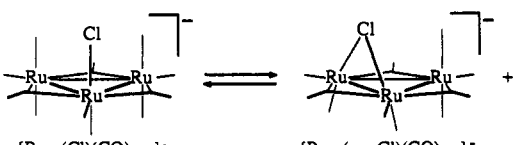

(1)

(1) (a) Anstock, M.; Taube, D.; Cross, D. C.; Ford, P. C. *J. Am. Chem. Soc.* **1984**, *106*, 3696–3697. (b) Darensbourg, D. L.; Gray, R. L.; Pala, M. *Organometallics* **1984**, *3*, 1928–1930. (c) Taube, D. J.; van Eldik, R.; Ford, P. C. *Organometallics* **1987**, *6*, 125–129 and references therein. (d) Taube, D. J.; Rokicki, A.; Anstock, M.; Ford, P. C. *Inorg. Chem.* **1987**, *26*, 526–530. (e) Bhaduri, S.; Khwaja, H.; Sharma, K.; Jones, P. G. *J. Chem. Soc., Chem. Commun.* **1989**, 515–516.

(2) (a) Szostak, S.; Strouse, C. E.; Kaesz, H. D. *J. Organomet. Chem.* **1980**, *191*, 243–260. (b) Mayr, A.; Lin, Y. C.; Boag, N. M.; Kaesz, H. D. *Inorg. Chem.* **1982**, *21*, 1704–1706. (c) Mayr, A.; Lin, Y. C.; Boag, N. M.; Kampe, C. E.; Knobler, C. B.; Kaesz, H. D. *Inorg. Chem.* **1984**, *23*, 4640–4645. (d) Boag, N. M.; Sieber, W. J.; Kampe, C. E.; Knobler, C. B.; Kaesz, H. D. *J. Organomet. Chem.* **1988**, *355*, 385–400.

(3) (a) Lavigne, G.; Kaesz, H. D. *J. Am. Chem. Soc.* **1984**, *106*, 4647–4648. (b) Han, S.-H.; Geoffroy, G. L.; Rheingold, A. L. *Inorg. Chem.* **1987**, *26*, 3426–3428. (c) Han, S.-H.; Geoffroy, G. L.; Dombek, B. D.; Rheingold, A. L. *Inorg. Chem.* **1988**, *27*, 4355–4361. (d) Han, S.-H.; Geoffroy, G. L. *Polyhedron* **1988**, *7*, 2331–2339. (e) Han, S.-H.; Song, J.-S.; Macklin, P. D.; Nguyen, S. T.; Geoffroy, G. L. *Organometallics* **1989**, *8*, 2127–2138. (f) Chin-Choy, T.; Harrison, W. T. A.; Stucky, G. D.; Keder, N.; Ford, P. C. *Inorg. Chem.* **1989**, *28*, 2028–2029. (g) Rivomanana, S.; Lavigne, G.; Lugan, N.; Bonnet, J.-J.; Yanez, R.; Mathieu, R. *J. Am. Chem. Soc.* **1989**, *111*, 8959–8960. (h) Rivomanana, S.; Lavigne, G.; Lugan, N.; Bonnet, J.-J. *Organometallics* **1991**, *10*, 2285–2297.

(4) (a) Zuffa, J. L.; Blohm, M. L.; Gladfelter, W. L. *J. Am. Chem. Soc.* **1986**, *108*, 552–553. (b) Zuffa, J. L.; Gladfelter, W. L. *J. Am. Chem. Soc.* **1986**, *108*, 4669–4671.

(5) For various catalytic systems involving $Ru_3(CO)_{12}$ as a precursor and anionic nucleophiles as promoters, see: (a) Dombek, B. D. *Organometallics* **1985**, *4*, 1707–1712 and references therein. (b) Dombek, B. D. *J. Organomet. Chem.* **1989**, *372*, 151–161 and references therein. (c) Kiso, Y.; Saeki, K. *J. Organomet. Chem.* **1986**, *309*, C26–C28. (d) Knifton, J. *J. Mol. Catal.* **1988**, *47*, 99–116 and references therein. (e) Knifton, J. In *Aspects of Homogeneous Catalysis*; Ugo, R., Ed; Reidel Publishing: 1988; Vol. 6, pp 1–58 and references therein. (f) Yoshida, S.-I.; Mori, S.; Kinoshita, H.; Watanabe, Y. *J. Mol. Catal.* **1987**, *42*, 215–227. (g) Ono, H.; Fujiwara, K.; Hashimoto, M.; Watanabe, H.; Yoshida, K. *J. Mol. Catal.* **1990**, *58*, 289–297. (h) Cenini, S.; Crotti, C.; Pizzotti, M.; Porta, F. *J. Org. Chem.* **1988**, *53*, 1243–1250 and references therein. (i) Bhaduri, S.; Khwaja, H.; Sharma, K.; Jones, P. G. *J. Chem. Soc., Chem. Commun.* **1989**, 515–516. (j) Bhaduri, S.; Khwaja, H.; Sapre, N.; Sharma, K.; Basu, A.; Jones, P. G.; Carpenter, G. *J. Chem. Soc., Dalton Trans.* **1990**, 1313–1321.

0276-7333/92/2311-1351$03.00/0

to determine whether other nucleophiles such as alkoxo, amido, or thiolato groups could experience similar bridge-opening reactions which may have mechanistic implications in homogeneous catalysis, as suggested by Basset and co-workers in the case of cluster-bound siloxo groups.[7]

Since a facile loss of the weakly coordinated alkoxo or amido groups might be expected in the case of ruthenium, we were led to devise a new series of activated clusters in which one of these groups would be anchored onto the metal framework by a functionalized arm. Keeping in mind the characteristics of the phenylpyridylphosphido group as a stabilizing ligand in triruthenium cluster complexes,[8] we were inclined to select the pyridyl group as a potential functionalized arm. It thus appeared that anions derived from 2-hydroxypyridine, 2-anilinopyridine, and 2-mercaptopyridine were interesting ligands to consider if one could find appropriate means to incorporate them into the cluster.

In this paper, we report full details of the high-yield syntheses of the trinuclear complexes derived from $Ru_3(CO)_{12}$ by incorporation of the hybrid ligands $X(C_5H_4N)^-$ (**a**, X = $N(C_6H_5)$; **b**, X = S; **c**, X = O), namely the anionic species $[Ru_3(\mu_i\text{-}\eta^2\text{-}X(C_5H_4N))(CO)_n]^-$ (**1a,c**), $i = 2$; $n = 10$; **2a–c**, $i = 3$; $n = 9$) and the corresponding neutral hydrido derivatives $Ru_3(\mu\text{-}H)(\mu_3\text{-}\eta^2\text{-}X(C_5H_4N))(CO)_9$ (**3a,b**). On the basis of the X-ray structures of PPN·**1c** and PPN·**2a** (PPN = $(C_6H_5)_3PNP(C_6H_5)_3^+$), we analyze the features which may account for the enhanced reactivity of these "lightly ligand-bridged" complexes. Furthermore, we report the details of the facile reaction of **3a,b** with diphenylacetylene, leading selectively to the reactive alkenyl complex $Ru_3(\mu_3\text{-}\eta^2\text{-}X(C_5H_4N))(\mu\text{-}(C_6H_5)CCH(C_6H_5))(CO)_8$ (**4a,b**) the structure of which has been determined by X-ray diffraction.

While our preliminary communication on this work was in press,[9] Riera and co-workers reported a preparation of compounds **3a**[10] and **3b**[11] based on a classical thermal route.

Results

Syntheses. As noted by M. I. Bruce in a recent review,[12] the lack of systematic high-yield synthetic routes to ruthenium clusters containing N-donor ligands has long been a major impediment to the development of their chemistry. In particular, various hybrid ligands containing the X—C=N– linkage (X = S, NR) are known to give complexes of the type $Ru_3(\mu\text{-}H)(\mu_3\text{-}XCR'{=}NR'')(CO)_9$ that have been isolated and structurally characterized for the first time by Jeannin and co-workers[13] in the case of the mercaptobenzothiazole ligand. However, such complexes

Scheme I. Principal Synthetic Methods (Abbreviations: PPN = $[(C_6H_5)_3PNP(C_6H_5)_3]^+$; Ph = C_6H_5; Py = C_5H_4N)

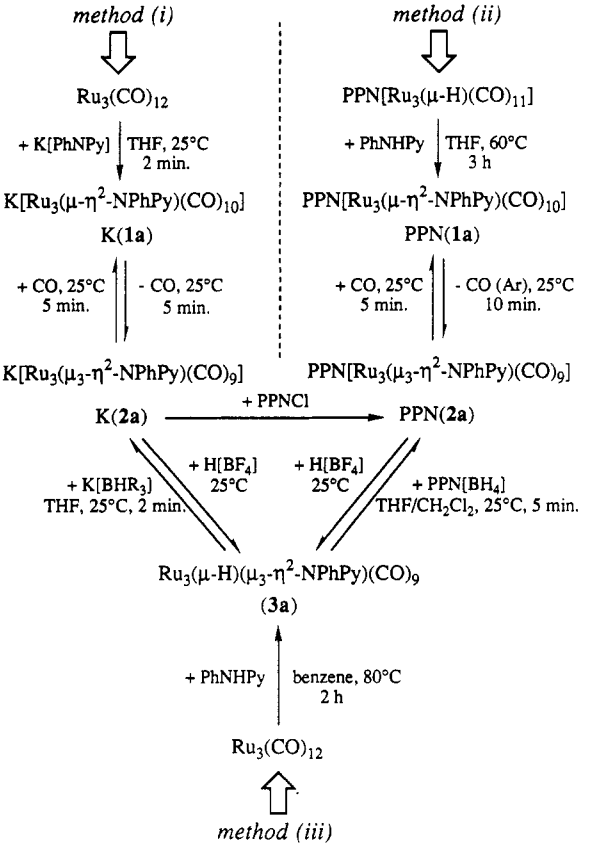

are generally not obtained in high yield via thermal routes. Proline and cysteine derivatives, which belong to a closely related ligand category, have been recently shown to react with $Ru_3(CO)_{12}$ under mild thermal activation (50–60 °C), yet requiring prolonged reaction times.[14] Thus, we have devised alternate methods which are applied to the hybrid ligands considered here, namely (**a**) 2-anilinopyridine, (**b**) 2-mercaptopyridine, and (**c**) 2-hydroxypyridine. A more common thermal route that applies only to 2-anilinopyridine is also described.

A. 2-Anilinopyridine Derivatives PPN·1a, PPN·2a, and 3a. The three principal synthetic methods described below are summarized in Scheme I, where possible interconversions between the different reaction products are also shown.

Method i. Deprotonation of hybrid ligands of this type by various bases has been widely used to incorporate them into organometallic complexes.[15] Surprisingly, such a procedure has not been used for trinuclear carbonyl clusters of the iron triad. Our method involves the addition of K-Selectride or related bases to 2-anilinopyridine, leading to the instantaneous formation of $K[N(C_6H_5)(C_5H_4N)]$. The reaction of this salt with $Ru_3(CO)_{12}$ at 25 °C gives the complex $K[Ru_3(\mu_3\text{-}\eta^2\text{-}N(C_6H_5)(C_5H_4N))(CO)_9]$ K·**2a**. A careful monitoring of the reaction by infrared spectroscopy indicates the transient formation of the intermediate K·**1a** which can be intercepted under 1

(6) For recent reviews dealing with nucleophilic activation of ruthenium carbonyl complexes, see: (a) Ford, P. C.; Rokicki, A. *Adv. Organomet. Chem.* **1988**, *28*, 139–217. (b) Lavigne, G.; Kaesz, H. D. In *Metal Clusters in Catalysis*; Gates, B.; Guczi, L.; Knözinger, H., Eds.; Elsevier: Amsterdam, 1986; Chapter 4, pp 43–88. (c) Lavigne, G. In *The Chemistry of Metal Clusters*; Shriver, D., Adams, R. D., Kaesz, H. D., Eds.; Verlag Chemie: 1990; Chapter 5, pp 201–302 and references therein.

(7) Choplin, A.; Besson, L.; D'Ornelas, R.; Sanchez-Delgado, R.; Basset, J. M. *J. Am. Chem. Soc.* **1988**, *110*, 2783–2787.

(8) (a) Lugan, N.; Lavigne, G.; Bonnet, J.-J. *Inorg. Chem.* **1986**, *25*, 7–9. (b) Lugan, N.; Lavigne, G.; Bonnet, J.-J. *Inorg. Chem.* **1987**, *26*, 585–590. (c) Lugan, N.; Lavigne, G.; Bonnet, J.-J.; Réau, R.; Neibecker, D.; Tkatchenko, I. *J. Am. Chem. Soc.* **1988**, *110*, 5369–5376.

(9) Lugan, N.; Laurent, F.; Lavigne, G.; Newcomb, T. P.; Liimatta, E. W.; Bonnet, J.-J. *J. Am. Chem. Soc.* **1990**, *112*, 8607–8609.

(10) Andreu, P. L.; Cabeza, J. A.; Riera, V.; Jeannin, Y.; Miguel, D. *J. Chem. Soc., Dalton Trans.* **1990**, 2201–2206.

(11) Andreu, P. L.; Cabeza, J. A.; Fernandez-Colinas, J. M.; Riera, V *J. Chem. Soc., Dalton Trans.* **1990**, 2927–2930.

(12) Bruce, M. I.; Cifuentes, M. P.; Humphrey, M. G. *Polyhedron.* **1991**, *10*, 277–322 and references therein.

(13) Jeannin, S.; Jeannin, Y.; Lavigne, G. *Inorg. Chem.* **1978**, *17*, 2103–2110.

(14) Süss-Fink, G.; Jenke, T.; Heitz, H.; Pellinghelli, M. A.; Tiripicchio, A. *J. Organomet. Chem.* **1989**, *379*, 311–323.

(15) (a) Fryzuk, M. D.; Montgomery, C. D. *Coord. Chem. Rev.* **1989**, *95*, 1–40 and references therein. (b) Cotton, F. A.; Niswander, R. H.; Sekutowski, J. C. *Inorg. Chem.* **1978**, *17*, 3541–3546. (c) Bancroft, D. P.; Cotton, F. A.; Falvello, L. R.; Schwotzer, W. *Inorg. Chem.* **1986**, *25*, 763–770. (d) Sherlock, S. J.; Cowie, M.; Singleton, E.; de V. Steyn, M. M. *J. Organomet. Chem.* **1989**, *361*, 353–367. (e) Ciriano, M. A.; Villaroya, B. E.; Oro, L.; Apreda, M. C.; Foces-Foces, C.; Cano, F. H. *J. Organomet. Chem.* **1989**, *366*, 377–389.

Table I. Crystal and Intensity Data for PPN[$Ru_3(\mu\text{-}\eta^2\text{-}O(C_5H_4N))(CO)_{10}$] (PPN•1c), PPN[$Ru_3(\mu_3\text{-}\eta^2\text{-}N(C_6H_5)(C_5H_4N))(CO)_9$] (PPN•2a), and $Ru_3(\mu_3\text{-}\eta^2\text{-}N(C_6H_5)(C_5H_4N))(\mu\text{-}(C_6H_5)CCH(C_6H_5))(CO)_8$•0.5$CH_2Cl_2$ (4a)

compound	PPN·1c	PPN·2a	4a
formula	$C_{51}H_{34}N_2O_{11}P_2Ru_3$	$C_{56}H_{39}N_2O_9P_2Ru_3$	$C_{33}H_{20}N_2O_8Ru_3$·0.5CH_2Cl_2
fw	1216.01	1263.10	918.21
a, Å	13.209 (1)	15.933 (2)	10.424 (1)
b, Å	18.149 (1)	17.163 (2)	18.795 (2)
c, Å	11.217 (2)	10.384 (2)	8.964 (1)
α, deg	102.371 (9)	102.69 (1)	93.97 (1)
β, deg	96.52 (1)	91.06 (1)	105.09 (1)
γ, deg	107.401 (7)	107.55 (1)	78.51 (1)
V, Å^3	2460 (10)	2630	1661 (5)
Z	2	2	2
ρ_{calcd}, g cm^{-3}	1.64	1.59	1.83
space group	C_i^1-$P\bar{1}$	C_i^1-$P\bar{1}$	C_i^1-$P\bar{1}$
T, °C	20	20	20
radiation (graphite monochrom)	λ(Mo Kα_1) = 0.7093 Å	λ(Mo Kα_1) = 0.7093 Å	λ(Mo Kα_1) = 0.7093 Å
linear abs coeff, cm^{-1}	10.15	8.64	13.76
abs corrections	numerical integration	empirical (Ψ-scan)	numerical integration
transmission factors	0.8873–0.6554	0.997–0.921	0.898–0.727
crystal shape	8 faces		6 faces
boundary faces and respective distances to crystal origin, cm	{100}, {10$\bar{1}$}, {010}, {1$\bar{1}$0}; 0.006, 0.021, 0.021, 0.019		{100}, {010}, {001}; 0.012, 0.004, 0.022
crystal volume, mm^3	0.029		0.009
receiving aperture, mm	4.0 × 4.0	4.0 × 4.0	4.0 × 4.0
take-off angle, deg	3.25	2.3	2.5
scan speed, deg min^{-1}	2.0	2.0	2.0
scan mode	ω–2θ	ω–2θ	ω–2θ
scan range, deg	0.85 below Kα_1 to 0.85 above Kα_2		
θ limit, deg	1–26	1–25	1–26.5
unique data used in final refinement, $F_o^2 > 3\sigma(F_o^2)$	7330	5665	5502
final no. of variables	382	364	436
R (on F_o, $F_o^2 > 3\sigma(F_o^2)$)[a]	0.042	0.042	0.023
R_w (on F_o, $F_o^2 > 3\sigma(F_o^2)$)[b]	0.043	0.042	0.025
weighting scheme	unit weights	$w = 1/\sigma^2$; $p = 0.02$[c]	
error in observ unit weight, Å^2	1.8	2.37	1.08

[a] $R = \sum||F_o| - |F_c||/\sum|F_o|$. [b] $R_w = [\sum w(|F_o| - |F_c|)^2/(\sum w|F_o|^2)]^{1/2}$. [c] $\sigma^2 = \sigma^2(F) + |p^2F^2|$.

atmosphere of carbon monoxide (vide infra). The anion **2a** is isolated and crystallized in 80–90% yield as the salt PPN·**2a** via metathesis with (PPN)Cl.

Method ii. Keeping in mind an earlier report on the enhanced substitutional lability of PPN[$Ru_3(\mu\text{-}H)(CO)_{11}$] relative to $Ru_3(CO)_{12}$,[16] we attempted the preparation of PPN·**2a** by reaction of 2-anilinopyridine with PPN[$Ru_3(\mu\text{-}H)(CO)_{11}$]. We found that the reaction proceeds cleanly at 60 °C in THF under reflux within 3 h, with a progressive color change of the solution from dark red to yellow. This method provides the salt PPN·**2a** in about 60% yield after recrystallization from acetone/ethanol mixtures. Trace amounts of the more soluble hydrido anion PPN[$Ru_4(\mu\text{-}H)_3(CO)_{12}$] are detected in the solution. Such a reaction may bear some relevance to the hydridic behavior of PPN[$Ru_3(\mu\text{-}H)(CO)_{11}$].[17]

Method iii. Unlike other ligands considered in this work (vide infra), 2-anilinopyridine reacts cleanly and almost quantitatively with $Ru_3(CO)_{12}$ in refluxing benzene within 2 h to give the complex $Ru(\mu\text{-}H)(\mu_3\text{-}\eta^2\text{-}N(C_6H_5)(C_5H_4N))(CO)_9$ (**3a**) in 85–90% yield. As indicated above, the compound has now also been prepared independently by Riera and co-workers (refluxing toluene, 45 min, 66% yield) and characterized by X-ray crystallography.[10] In contrast to the observation that complexes of this type are not deprotonated by triethylamine or potassium methoxide,[18] we find that **3a** is instantaneously deprotonated upon reaction with $(PPN)BH_4$ to give the anion PPN·**2a** (90% yield). Conversely, titration of **2a** (derived from any of the above synthetic methods) with CF_3COOH provides the neutral complex **3a** in quantitative spectroscopic yield.

Trapping the Intermediate PPN·1a. As noted above, an intermediate is detected by infrared spectroscopy when K·**2a** is prepared under the ambient temperature conditions of method i. Its infrared absorption bands are maximized when a THF solution of **2a** is saturated with CO at 25 °C. Conversely, it cleanly reverts to **2a** within few minutes at 25 °C under a stream of inert gas. Due to the fate of this intermediate in the absence of carbon monoxide, we did not make a further attempt to isolate it. Its formulation as the anionic CO adduct $[Ru_3(\mu\text{-}\eta^2\text{-}N(C_6H_5)(C_5H_4N))(CO)_{10}]^-$ (**1a**) rests on the analogy of its infrared ν(CO) absorption bands with those of the more stable analogue **1c** which has been isolated and fully characterized as its PPN salt (vide infra).

B. 2-Mercaptopyridine Derivatives PPN·2b and 3b. Method i described above applies equally well to the preparation of PPN[$Ru_3(\mu_3\text{-}\eta^2\text{-}S(C_5H_4N))(CO)_9$] (PPN·**2b**) from $Ru_3(CO)_{12}$ and 2-mercaptopyridine. Although it is very likely that the reaction also proceeds via the formation of the elusive intermediate decacarbonyl species K[$Ru_3(\mu\text{-}\eta^2\text{-}S(C_5H_4N))(CO)_{10}$], the latter was not intercepted under the experimental conditions of this work.

In an attempt to extend the scope of catalytic halide-promoted substitution reactions of $Ru_3(CO)_{12}$,[3a] we were prompted to examine the alternate possibility of assisting the incorporation of 2-mercaptopyridine into $Ru_3(CO)_{12}$ by addition of catalytic amounts of (PPN)Cl. In fact, we found that, just as in the case of the incorporation of alkynes,[3g,h] the reaction requires a stoichiometric amount of (PPN)Cl. Once the intermediate complex PPN[Ru_3-

(16) Taube, D. J.; Ford, P. C. *Organometallics* **1986**, *5*, 99–104.
(17) (a) Bricker, J. C.; Nagel, C. C.; Shore, S. G. *J. Am. Chem. Soc.* **1985**, *107*, 377–384. (b) Payne, M. W.; Leussing, D. L.; Shore, S. G. *J. Am. Chem. Soc.* **1987**, *109*, 617–618. (c) Payne, M. W.; Leussing, D. L.; Shore, S. G. *Organometallics* **1991**, *10*, 574–580. (d) Barrat, D. S.; Cole Hamilton, D. J. *J. Chem. Soc., Chem. Commun.* **1985**, 1559–1560. (e) Lavigne, G.; Lugan, N.; Bonnet, J.-J. *Inorg. Chem.* **1987**, *26*, 2345–2347.
(18) Andreu, P. L.; Cabeza, J. A.; Riera, V.; Bois, C.; Jeannin, Y. *J. Chem. Soc., Dalton Trans.* **1990**, 3347–3353.

Table II. Fractional Atomic Coordinates and Isotropic or Equivalent Temperature Factors (Å² × 100) for the Complex PPN•1c with Esd's in Parentheses

atom	x/a	y/b	z/c	U_{eq}/U_{iso}
Ru(1)	0.42027 (3)	0.81237 (2)	0.23679 (5)	4.81 (8)
Ru(2)	0.42269 (3)	0.81700 (3)	0.49334 (4)	4.47 (7)
Ru(3)	0.43753 (3)	0.68259 (2)	0.31802 (4)	3.74 (6)
P(1)	0.0404 (1)	0.27732 (7)	0.2667 (1)	3.7 (2)
P(2)	0.1401 (1)	0.25137 (8)	0.0337 (1)	3.7 (2)
C(1)	0.3926 (6)	0.8613 (4)	0.1089 (7)	8 (1)
O(1)	0.3750 (6)	0.8919 (4)	0.0351 (6)	14 (2)
C(2)	0.5664 (5)	0.8672 (4)	0.2599 (7)	7 (1)
O(2)	0.6573 (4)	0.8987 (3)	0.2724 (6)	11 (1)
C(3)	0.4038 (4)	0.8987 (3)	0.3843 (6)	5 (1)
O(3)	0.3886 (4)	0.9596 (2)	0.4031 (5)	7.3 (9)
C(4)	0.4169 (5)	0.8755 (4)	0.6505 (6)	7 (1)
O(4)	0.4123 (5)	0.9131 (4)	0.7436 (5)	11 (1)
C(5)	0.5792 (5)	0.8638 (3)	0.5352 (6)	6 (1)
O(5)	0.6701 (4)	0.8906 (3)	0.5666 (5)	8 (1)
C(6)	0.4349 (4)	0.7032 (3)	0.5090 (5)	4.8 (9)
O(6)	0.4396 (4)	0.6700 (3)	0.5868 (4)	7.6 (9)
C(7)	0.4369 (4)	0.5759 (3)	0.2833 (5)	4.1 (8)
O(7)	0.4396 (3)	0.5124 (2)	0.2653 (4)	5.9 (7)
C(8)	0.5886 (4)	0.7190 (3)	0.3515 (6)	5 (1)
O(8)	0.6808 (3)	0.7412 (3)	0.3696 (5)	7.4 (9)
C(9)	0.4410 (4)	0.7075 (3)	0.1391 (6)	4.8 (9)
O(9)	0.4540 (3)	0.6786 (3)	0.0414 (4)	6.3 (8)
C(10)	0.2660 (5)	0.7735 (3)	0.4689 (5)	5 (1)
O(10)	0.1759 (3)	0.7536 (3)	0.4658 (4)	6.8 (9)
O(11)	0.2518 (3)	0.7464 (2)	0.1956 (3)	4.9 (6)
N(1)	0.2620 (3)	0.6404 (2)	0.2735 (4)	3.9 (7)
C(12)	0.2066 (4)	0.6782 (3)	0.2139 (5)	4.3 (8)
C(13)	0.0919 (5)	0.6415 (4)	0.1730 (6)	6 (1)
C(14)	0.0385 (5)	0.5737 (4)	0.2012 (7)	6 (1)
C(15)	0.0957 (5)	0.5382 (4)	0.2688 (7)	6 (1)
C(16)	0.2049 (5)	0.5727 (3)	0.3013 (6)	5 (1)
N(2)	0.0852 (4)	0.2753 (3)	0.1441 (4)	5.9 (9)
C(21)	0.0406 (3)	0.1948 (2)	−0.1047 (3)	4.2 (1)
C(22)	−0.0607 (3)	0.1462 (2)	−0.0950 (3)	5.8 (1)
C(23)	−0.1383 (3)	0.1028 (2)	−0.2020 (3)	6.7 (2)
C(24)	−0.1148 (3)	0.1079 (2)	−0.3187 (3)	6.8 (2)
C(25)	−0.0136 (3)	0.1565 (2)	−0.3284 (3)	6.7 (2)
C(26)	0.0641 (3)	0.2000 (2)	−0.2214 (3)	5.5 (1)
C(31)	0.2194 (3)	0.3414 (2)	0.0021 (3)	3.7 (1)
C(32)	0.3119 (3)	0.3457 (2)	−0.0487 (3)	4.6 (1)
C(33)	0.3704 (3)	0.4164 (2)	−0.0745 (3)	5.4 (1)
C(34)	0.3361 (3)	0.4829 (2)	−0.0497 (3)	5.5 (1)
C(35)	0.2435 (3)	0.4786 (2)	0.0011 (3)	5.6 (1)
C(36)	0.1851 (3)	0.4078 (2)	0.0269 (3)	4.7 (1)
C(41)	0.2254 (3)	0.1934 (2)	0.0579 (4)	4.5 (1)
C(42)	0.3251 (3)	0.2298 (2)	0.1389 (4)	6.7 (2)
C(43)	0.3926 (3)	0.1854 (2)	0.1572 (4)	8.4 (2)
C(44)	0.3603 (3)	0.1045 (2)	0.0945 (4)	9.2 (2)
C(45)	0.2606 (3)	0.0680 (2)	0.0136 (4)	9.5 (2)
C(46)	0.1932 (3)	0.1125 (2)	−0.0047 (4)	7.0 (2)
C(51)	0.1406 (3)	0.3396 (2)	0.4006 (2)	3.9 (1)
C(52)	0.2371 (3)	0.3921 (2)	0.3860 (2)	4.9 (1)
C(53)	0.3131 (3)	0.4429 (2)	0.4903 (2)	5.6 (1)
C(54)	0.2928 (3)	0.4413 (2)	0.6092 (2)	5.8 (1)
C(55)	0.1963 (3)	0.3888 (2)	0.6238 (2)	5.4 (1)
C(56)	0.1203 (3)	0.3380 (2)	0.5195 (2)	4.8 (1)
C(61)	−0.0076 (2)	0.1811 (2)	0.2961 (4)	4.2 (1)
C(62)	0.0679 (2)	0.1446 (2)	0.3242 (4)	6.7 (2)
C(63)	0.0337 (2)	0.0682 (2)	0.3433 (4)	8.0 (2)
C(64)	−0.0762 (2)	0.0283 (2)	0.3343 (4)	7.6 (2)
C(65)	−0.1517 (2)	0.0648 (2)	0.3062 (4)	7.4 (2)
C(66)	−0.1174 (2)	0.1411 (2)	0.2871 (4)	5.6 (1)
C(71)	−0.0687 (3)	0.3166 (2)	0.2559 (3)	3.9 (1)
C(72)	−0.1338 (3)	0.2978 (2)	0.1392 (3)	6.7 (2)
C(73)	−0.2224 (3)	0.3241 (2)	0.1262 (3)	8.4 (2)
C(74)	−0.2460 (3)	0.3692 (2)	0.2299 (3)	7.7 (2)
C(75)	−0.1809 (3)	0.3880 (2)	0.3466 (3)	6.9 (2)
C(76)	−0.0923 (3)	0.3617 (2)	0.3596 (3)	5.2 (1)

(μ-Cl)$(CO)_{10}$] is formed, it reacts rapidly with 2-mercaptopyridine to give $Ru_3(\mu\text{-H})(\mu_3\text{-}\eta^2\text{-S}(C_5H_4N))(CO)_9$ (**3b**) with concomitant elimination of (PPN)Cl. Though such a reaction is potentially catalytic, the halide anion released in solution tends to deprotonate the hydrido complex,[3e,g] giving variable amounts of the corresponding anion $[Ru_3(\mu_3\text{-}\eta^2\text{-S}(C_5H_4N))(CO)_9]^-$ (**2b**). The acid–base equilibrium between these species can be subsequently shifted toward the formation of the neutral derivative **3b** upon acidification with excess CF_3COOH or, alternatively, toward the formation of the anionic derivative **2b** by addition of an excess of (PPN)Cl. Though such a synthetic procedure is conceptually interesting, it is not of practical use here, due to the simplicity of the previous one.

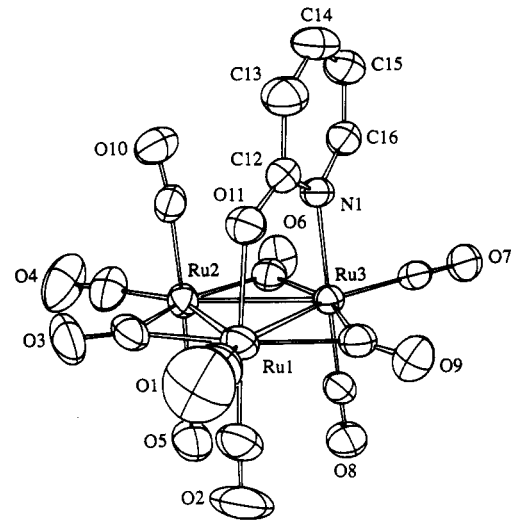

Figure 1. Perspective view of the anion $[Ru_3(\mu\text{-}\eta^2\text{-O}(C_5H_4N))(CO)_{10}]^-$ (**1c**). Thermal ellipsoids are shown at 50% probability level.

The thermal route to the neutral hydrido derivative $Ru_3(\mu\text{-H})(\mu_3\text{-}\eta^2\text{-S}(C_5H_4N))(CO)_9$ (**3b**) is rather inefficient, as indicated by the low yields of **3b** (29%) obtained by other authors in such a reaction, leading principally to polymeric products.[11] By contrast, we find that methods i and ii are highly efficient. The best one is method i, providing quantitative yields of K·**2b** (first) and **3b** (after protonation) within few minutes.

C. 2-Hydroxypyridine Derivatives PPN·1c and PPN·2c. Alcohols do not currently react with $Ru_3(CO)_{12}$, except in specific cases[19] or under drastic[20] conditions. The thermal reaction between $Ru_3(CO)_{12}$ and 2-hydroxypyridine is known to give only polymeric products.[11] By contrast, methods i and ii above allow facile incorporation of this ligand without any observable cluster fragmentation. Furthermore, we have found that addition of OPy^- to $Ru_3(CO)_{12}$ leads to the decacarbonyl derivative $[Ru_3(\mu\text{-}\eta^2\text{-O}(C_5H_4N))(CO)_{10}]^-$ (**1c**) exclusively instead of **2c**, even at 60 °C in refluxing THF. Similarly, the reaction of 2-hydroxypyridine with $PPN[Ru_3(\mu\text{-H})(CO)_{11}]$ (method ii), gives only PPN·**1c**, with no evidence for the formation of PPN·**2c**. This is a clear indication that the equilibrium between the two anionic species is shifted toward the formation of the more stable decacarbonyl derivative. Decarbonylation of PPN·**1c** to give PPN·**2c** is rather tedious and is only partially observed by IR spectroscopy after 2–3 h in THF at 60 °C under a stream of inert gas. Thus, we have not made further attempts to isolate PPN·**2c**.

(19) (a) Aime, S.; Botta, M.; Gobetto, R.; Osella, D.; Padovan, F. *J. Chem. Soc., Dalton Trans.* **1987**, 253–254. (b) Santini, C. C.; Basset, J. M.; Fontal, B.; Krause, J.; Shore, S. G.; Charrier, C. *J. Chem. Soc., Chem. Commun.* **1987**, 512–513. (c) Johnson, B. F. G.; Lewis, J.; Mace, J. M.; Raithby, P. R.; Vargas, M. D. *J. Organomet. Chem.* **1987**, *321*, 409–416.

(20) (a) Bohle, S.; Vahrenkamp, H. *Angew. Chem., Int. Ed. Engl.* **1990**, *29*, 198–199.

Table III. Selected Interatomic Distances (Å) for PPN•1c with Esd's in Parentheses[a]

		Ru–Ru			
		Ru(1)–Ru(2)	2.8571 (9)		
Ru(1)–Ru(3)	2.7611 (7)			Ru(2)–Ru(3)	2.8592 (7)
		Ru–C (Terminal Carbonyl Groups in Equatorial Position)			
Ru(1)–C(1)	1.898 (8)			Ru(2)–C(4)	1.876 (7)
		Ru(3)–C(7)	1.888 (6)		
		Ru–C (Terminal Carbonyl Groups in Axial Position)			
Ru(1)–C(2)	1.846 (6)			Ru(2)–C(5)	1.942 (6)
		Ru(3)–C(8)	1.869 (5)		
				Ru(2)–C(10)	1.945 (6)
		Ru–C (Bridging Carbonyl Groups in Equatorial Position)			
Ru(1)–C(3)	2.101 (6)			Ru(2)–C(3)	2.165 (7)
Ru(1)–C(9)	2.095 (6)			Ru(2)–C(6)	2.160 (6)
Ru(3)–C(9)	2.151 (7)			Ru(3)–C(6)	2.100 (6)
		Ru–O			
Ru(1)–O(11)	2.129 (3)				
		Ru–N			
Ru(3)–N(1)	2.173 (4)				
		α-Pyridone Ligand			
O(11)–C(12)	1.276 (6)	C(12)–N(1)	1.355 (8)	C(12)–C(13)	1.435 (8)
C(13)–C(14)	1.34 (1)	C(14)–C(15)	1.39 (1)	C(15)–C(16)	1.359 (8)
C(16)–N(1)	1.357 (7)				
		C–O (Terminal Carbonyl Groups in Equatorial Position)			
C(1)–O(1)	1.13 (1)			C(4)–O(4)	1.137 (9)
		C(7)–O(7)	1.139 (7)		
		C–O (Terminal Carbonyl Groups in Axial Position)			
C(2)–O(2)	1.143 (8)			C(5)–O(5)	1.134 (6)
		C(8)–O(8)	1.142 (7)		
C(10)–O(10)	1.130 (7)				
		C–O (Bridging Carbonyl Groups in Equatorial Position)			
		C(3)–O(3)	1.162 (8)		
C(9)–O(9)	1.164 (7)			C(6)–O(6)	1.168 (8)
		Bis(triphenylphosphoranylidene)ammonium Cation, PPN^+			
P(1)–N(2)	1.555 (5)			P(2)–N(2)	1.552 (5)
P(1)–C(51)	1.792 (3)			P(2)–C(21)	1.799 (3)
P(1)–C(61)	1.788 (4)			P(2)–C(31)	1.789 (3)
P(1)–C(71)	1.792 (5)			P(2)–C(41)	1.793 (5)

[a] Phenyl rings treated as rigid groups: C–C = 1.395 Å, C–H = 0.97 Å.

Finally, all attempts to protonate PPN·1c at low temperatures led to the formation of $Ru_3(CO)_{12}$ as the main product, thereby suggesting that protonation takes place at the oxygen atom of the ligand and promotes its decoordination.

D. Structural Characterization of PPN[$Ru_3(\mu$-η^2-O(C_5H_4N))$(CO)_{10}$] (PPN·1c) and PPN[$Ru_3(\mu_3$-η^2-N(C_6H_5)(C_5H_4N))$(CO)_9$] (PPN·2a). The X-ray structures of PPN·1c and PPN·2a have been determined. A perspective view of the anionic molecular unit of PPN·1c is shown in Figure 1. It consists of a triangular arrangement of ruthenium atoms. The μ-η^2-O(C_5H_4N) ligand occupies two axial coordination sites of the metal triangle and is linked through both the oxygen atom (Ru(1)–O(11) = 2.129 (3) Å) and the pyridyl nitrogen atom (Ru(3)–N(1) = 2.173 (4) Å). The supported metal–metal edge Ru(1)–Ru(3) is found slightly shorter than unsupported ones (Ru(1)–Ru(2) = 2.8571 (9) Å; Ru(1)–Ru(3) = 2.7611 (7) Å; Ru(2)–Ru(3) = 2.8592 (7) Å). The ligand shell of the cluster is completed by 10 carbonyl groups. Three of the equatorial carbonyl groups are in slightly asymmetric bridging position. Such a CO distribution is similar to that found in a few relevant anionic complexes such as PPN[$Ru_3(\mu$-η^2-HCOO)$(CO)_{10}$],[21] PPh_4[$Ru_3(\mu$-η^2-PhNCHO)$(CO)_{10}$],[1e] and [PPN]$_2$[$Ru_3(\mu$-η^2-CN)$(CO)_{10}]_2$[22] and also in a few neutral species containing nitrogen-donor atoms, such as $Ru_3(\mu$-η^2-napy)$(CO)_{10}$ (napy = 1,8-naphthyridine).[23] The

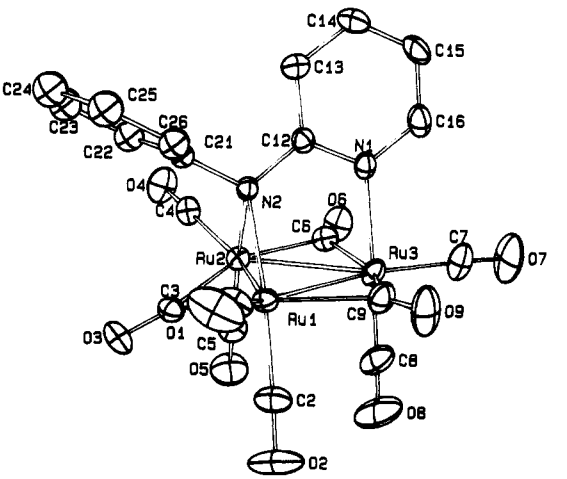

Figure 2. Perspective view of the anion [$Ru_3(\mu_3$-η^2-N(C_6H_5)(C_5H_4N))$(CO)_9]^-$ (**2a**). Thermal ellipsoids are shown at 30% probability level.

(21) Darensbourg, D. J.; Pala, M.; Waller, J. *Organometallics* **1983**, *2*, 1285–1291.

(22) Lavigne, G.; Lugan, N.; Bonnet, J.-J. *J. Chem. Soc., Chem. Commun.* **1987**, 957–958.

(23) Cabeza, J. A.; Oro, L. A.; Tiripicchio, A.; Tiripicchio Camellini, M. *J. Chem. Soc., Dalton Trans.* **1988**, 1437–1444.

Table IV. Selected Bond Angles (deg) for PPN•1c with Esd's in Parentheses

		Ru–Ru–Ru			
		Ru(1)–Ru(3)–Ru(2)	61.08 (2)		
Ru(2)–Ru(1)–Ru(3)	61.15 (2)			Ru(1)–Ru(2)–Ru(3)	57.76 (1)
		Ru–Ru–O (α-Pyridone)			
Ru(2)–Ru(1)–O(11)	89.6 (1)			Ru(3)–Ru(1)–O(11)	83.7 (1)
		Ru–Ru–N (α-Pyridone)			
Ru(1)–Ru(3)–N(1)	84.1 (1)			Ru(2)–Ru(3)–N(1)	86.8 (1)
		Ru–Ru–CO (Axial Carbonyls)			
Ru(3)–Ru(1)–C(2)	97.2 (2)			Ru(3)–Ru(2)–C(5)	90.8 (2)
Ru(2)–Ru(1)–C(2)	94.5 (2)			Ru(1)–Ru(2)–C(5)	92.3 (2)
Ru(1)–Ru(3)–C(8)	94.2 (2)			Ru(2)–Ru(3)–C(8)	93.9 (2)
Ru(1)–Ru(2)–C(10)	93.2 (2)			Ru(3)–Ru(2)–C(10)	93.4 (2)
		O–Ru–CO			
O(11)–Ru(1)–C(1)	87.0 (2)			O(11)–Ru(1)–C(2)	175.7 (3)
O(11)–Ru(1)–C(3)	92.6 (2)			O(11)–Ru(1)–C(9)	86.5 (2)
		N–Ru–CO			
N(1)–Ru(3)–C(7)	90.3 (2)			N(1)–Ru(3)–C(8)	178.3 (2)
N(1)–Ru(3)–C(6)	90.9 (2)			N(1)–Ru(3)–C(9)	89.2 (2)
		CO–Ru–CO (Adjacent Carbonyl Ligands Only)			
C(1)–Ru(1)–C(2)	90.3 (3)			C(4)–Ru(2)–C(5)	88.5 (3)
C(3)–Ru(1)–C(2)	91.0 (3)			C(3)–Ru(2)–C(5)	94.2 (2)
C(9)–Ru(1)–C(2)	90.9 (2)			C(6)–Ru(2)–C(5)	89.7 (2)
C(9)–Ru(3)–C(7)	102.2 (2)			C(6)–Ru(3)–C(7)	99.6 (2)
C(9)–Ru(3)–C(8)	89.1 (2)			C(6)–Ru(3)–C(8)	90.8 (2)
C(1)–Ru(1)–C(3)	96.8 (3)			C(4)–Ru(2)–C(3)	99.8 (3)
C(1)–Ru(1)–C(9)	102.8 (3)			C(4)–Ru(2)–C(6)	108.5 (3)
C(3)–Ru(2)–C(10)	88.3 (2)			C(4)–Ru(2)–C(10)	86.1 (2)
C(6)–Ru(2)–C(10)	90.5 (2)			C(7)–Ru(3)–C(8)	89.8 (2)
		Ru–C–O (Terminal Carbonyl Ligands in Equatorial Position)			
Ru(1)–C(1)–O(1)	178.0 (7)			Ru(2)–C(4)–O(4)	177.2 (8)
		Ru(3)–C(7)–O(7)	177.7 (4)		
		Ru–C–O (Terminal Carbonyl Ligands in Axial Position)			
Ru(1)–C(2)–O(2)	177.7 (7)			Ru(2)–C(5)–O(5)	175.9 (6)
		Ru(3)–C(8)–O(8)	178.7 (6)		
				Ru(2)–C(10)–O(10)	173.0 (5)
		Ru–C–O (Bridging Carbonyl Ligands in Equatorial Position)			
Ru(1)–C(3)–O(3)	140.1 (5)			Ru(2)–C(3)–O(3)	135.8 (5)
Ru(1)–C(9)–O(9)	140.1 (5)			Ru(2)–C(6)–O(6)	137.8 (4)
Ru(3)–C(9)–O(9)	138.6 (5)			Ru(3)–C(6)–O(6)	137.9 (5)
		α-Pyridone (Intramolecular Angles)			
O(11)–C(12)–N(1)	122.7 (4)			O(11)–C(12)–C(13)	118.2 (6)
N(1)–C(12)–C(13)	119.0 (5)			N(1)–C(16)–C(15)	124.3 (6)
C(12)–C(13)–C(14)	120.7 (7)			C(14)–C(15)–C(16)	118.2 (6)
C(12)–N(1)–C(16)	118.1 (4)			C(13)–C(14)–C(15)	119.4 (6)
		Bis(triphenylphosphoranylidene)ammonium Cation, PPN^+			
		P(1)–N(2)–P(2)	161.7 (4)		
N(2)–P(1)–C(51)	112.3 (2)			N(2)–P(2)–C(21)	110.8 (2)
N(2)–P(1)–C(61)	113.2 (2)			N(2)–P(2)–C(31)	107.8 (2)
N(2)–P(1)–C(71)	108.0 (2)			N(2)–P(2)–C(41)	115.4 (3)

coordination mode observed for the pyridonate ligand in our complex is analogous to that predicted by Deeming and co-workers[24] and Johnson, Lewis, and co-workers[25] for the partially characterized osmium pyridonate derivative $Os_3(\mu\text{-H})(\mu\text{-}\eta^2\text{-O}(C_5H_4N))(CO)_{10}$. Apart from this, few osmium carbonyl complexes involving a terminal amido group[26] or a terminal thiolato group[27] are known.

A perspective view of the anionic molecular unit of **PPN·2a** is shown in Figure 2. Clearly, the principal change with respect to the structural type described above is that the amido nitrogen atom is occupying a bridging position across the metal–metal edge Ru(1)–Ru(2). The latter is found to be significantly shorter than the two others (Ru(1)–Ru(2) = 2.668 (1) Å; Ru(1)–Ru(3) = 2.783 (1) Å; Ru(2)–Ru(3) = 2.795 (1) Å).

E. Reaction of $Ru_3(\mu\text{-H})(\mu_3\text{-}\eta^2\text{-X}(C_5H_4N))(CO)_9$ (3a,b) with Alkynes: Formation of the Alkenyl Derivatives $Ru_3(\mu_3\text{-}\eta^2\text{-X}(C_5H_4N))((\mu\text{-}(C_6H_5)CCH(C_6H_5))(CO)_8$ (4a,b). Keeping in mind detailed studies by Kaesz and co-workers[28] on the edge double-bridged complexes $Ru_3(\mu\text{-H})(\mu\text{-Cl})(CO)_{10}$ and $Ru_3(\mu\text{-H})(\mu\text{-O=CR})(CO)_{10}$, we were interested in determining whether the hydrido species $Ru_3(\mu\text{-H})(\mu_3\text{-}\eta^2\text{-X}(C_5H_4N))(CO)_9$ (**3a,b**) would exhibit a closely related substitutional lability. We[9] and others[29] observed that complex **3a** reacts within

(24) (a) Deeming, A. J.; Peters, R.; Hursthouse, M. B.; Backer-Dirks, J. D. J. *J. Chem. Soc., Dalton Trans.* **1982**, 1205–1211. (b) Deeming, A. J.; Peters, R. *J. Organomet. Chem.* **1982**, *235*, 221–226.

(25) Burgess, K.; Johnson, B. F. G.; Lewis, J. *J. Organomet. Chem.* **1982**, *233*, C55-C58.

(26) Süss-Fink, G.; Khan, L.; Raithby, P. R. *J. Organomet. Chem.* **1982**, *228*, 179–189.

(27) Adams, R. D.; Dawoodi, Z.; Foust, D. F.; Segmuller, B. E. *Organometallics* **1983**, *2*, 315–323.

(28) (a) Kampe, C. E.; Boag, N. M.; Knobler, C. B.; Kaesz, H. D. *Inorg. Chem.* **1984**, *23*, 1390–1397. (b) Kampe, C. E.; Kaesz, H. D. *Inorg. Chem.* **1984**, *23*, 4646–4653.

(29) Andreu, P. L.; Cabeza, J. A.; Riera, V.; Bois, C.; Jeannin, Y. *J. Organomet. Chem.* **1990**, *384*, C25-C28.

Table V. Fractional Atomic Coordinates and Isotropic or Equivalent Temperature Factors (Å² × 100) for the Complex PPN•2a with Esd's in Parentheses

atom	x/a	y/b	z/c	U_{eq}/U_{iso}
Ru(1)	0.30061 (3)	0.21063 (3)	0.39566 (5)	3.32 (9)
Ru(2)	0.43788 (3)	0.15191 (3)	0.36428 (5)	3.52 (9)
Ru(3)	0.46505 (4)	0.31387 (3)	0.52024 (5)	3.7 (1)
N(1)	0.3887 (3)	0.2186 (3)	0.2308 (5)	3.0 (8)
N(2)	0.4860 (3)	0.3508 (3)	0.3347 (5)	3.4 (9)
C(1)	0.1927 (5)	0.2107 (4)	0.3207 (7)	5 (1)
O(1)	0.1244 (4)	0.2112 (4)	0.2838 (7)	10 (2)
C(2)	0.2421 (5)	0.1876 (5)	0.5407 (8)	6 (2)
O(2)	0.2005 (5)	0.1723 (5)	0.6263 (6)	12 (2)
C(3)	0.3015 (4)	0.0833 (4)	0.3346 (6)	4 (1)
O(3)	0.2537 (3)	0.0153 (3)	0.3165 (5)	6 (1)
C(4)	0.4984 (4)	0.0887 (4)	0.2529 (7)	4 (1)
O(4)	0.5384 (4)	0.0513 (3)	0.1912 (6)	7 (1)
C(5)	0.4492 (5)	0.0978 (5)	0.4973 (8)	6 (2)
O(5)	0.4535 (4)	0.0642 (4)	0.5791 (6)	10 (1)
C(6)	0.5540 (5)	0.2471 (4)	0.4605 (6)	4 (1)
O(6)	0.6284 (3)	0.2542 (3)	0.4786 (5)	6 (1)
C(7)	0.5498 (5)	0.4110 (5)	0.6199 (8)	6 (2)
O(7)	0.6048 (4)	0.4656 (4)	0.6859 (7)	9 (2)
C(8)	0.4439 (5)	0.2784 (5)	0.6768 (8)	6 (2)
O(8)	0.4308 (5)	0.2556 (5)	0.7720 (6)	12 (2)
C(9)	0.3443 (4)	0.3393 (4)	0.5043 (7)	5 (1)
O(9)	0.3109 (3)	0.3905 (3)	0.5389 (6)	8 (1)
C(12)	0.4449 (4)	0.2967 (4)	0.2212 (6)	3 (1)
C(13)	0.4598 (5)	0.3195 (4)	0.0989 (7)	5 (1)
C(14)	0.5157 (5)	0.3974 (5)	0.0963 (8)	6 (2)
C(15)	0.5577 (5)	0.4518 (4)	0.2135 (8)	6 (2)
C(16)	0.5413 (4)	0.4267 (4)	0.3282 (8)	5 (1)
C(21)	0.3407 (3)	0.1703 (3)	0.1029 (4)	3.2 (1)
C(22)	0.3644 (3)	0.1037 (3)	0.0269 (4)	5.3 (2)
C(23)	0.3172 (3)	0.0587 (3)	−0.0949 (4)	5.9 (2)
C(24)	0.2464 (3)	0.0802 (3)	−0.1406 (4)	6.3 (2)
C(25)	0.2227 (3)	0.1468 (3)	−0.0646 (4)	6.1 (2)
C(26)	0.2698 (3)	0.1918 (3)	0.0572 (4)	4.8 (2)
P(1)	0.0256 (1)	0.7269 (1)	0.0258 (2)	3.2 (3)
P(2)	0.1457 (1)	0.7249 (1)	−0.1857 (2)	3.8 (3)
N(3)	0.0561 (3)	0.7204 (3)	−0.1184 (5)	3.9 (9)
C(31)	0.0283 (3)	0.8317 (3)	0.1046 (4)	3.5 (2)
C(32)	0.0680 (3)	0.8977 (3)	0.0457 (4)	5.2 (2)
C(33)	0.0710 (3)	0.9796 (3)	0.1070 (4)	6.7 (2)
C(34)	0.0343 (3)	0.9953 (3)	0.2271 (4)	6.4 (2)
C(35)	−0.0054 (3)	0.9293 (3)	0.2860 (4)	5.9 (2)
C(36)	−0.0084 (3)	0.8474 (3)	0.2247 (4)	4.7 (2)
C(41)	0.0878 (3)	0.6905 (2)	0.1301 (4)	3.6 (2)
C(42)	0.0839 (3)	0.6062 (2)	0.0920 (4)	4.9 (2)
C(43)	0.1370 (3)	0.5755 (2)	0.1623 (4)	6.1 (2)
C(44)	0.1942 (3)	0.6290 (2)	0.2708 (4)	7.0 (2)
C(45)	0.1982 (3)	0.7133 (2)	0.3090 (4)	7.6 (3)
C(46)	0.1450 (3)	0.7440 (2)	0.2386 (4)	5.4 (2)
C(51)	−0.0872 (3)	0.6624 (3)	0.0124 (4)	3.6 (2)
C(52)	−0.1399 (3)	0.6483 (3)	−0.1045 (4)	4.4 (2)
C(53)	−0.2296 (3)	0.6028 (3)	−0.1151 (4)	6.1 (2)
C(54)	−0.2665 (3)	0.5713 (3)	−0.0089 (4)	7.5 (3)
C(55)	−0.2138 (3)	0.5854 (3)	0.1079 (4)	8.1 (3)
C(56)	−0.1241 (3)	0.6310 (3)	0.1185 (4)	6.0 (2)
C(61)	0.1386 (3)	0.6236 (3)	−0.2862 (4)	4.1 (2)
C(62)	0.0618 (3)	0.5562 (3)	−0.2937 (4)	5.1 (2)
C(63)	0.0560 (3)	0.4768 (3)	−0.3706 (4)	6.8 (2)
C(64)	0.1270 (3)	0.4649 (3)	−0.4400 (4)	7.0 (2)
C(65)	0.2038 (3)	0.5323 (3)	−0.4325 (4)	7.2 (2)
C(66)	0.2096 (3)	0.6117 (3)	−0.3556 (4)	6.2 (2)
C(71)	0.1579 (2)	0.7952 (3)	−0.2936 (5)	3.9 (2)
C(72)	0.0809 (2)	0.8051 (3)	−0.3438 (5)	5.6 (2)
C(73)	0.0860 (2)	0.8587 (3)	−0.4288 (5)	7.3 (2)
C(74)	0.1681 (2)	0.9024 (3)	−0.4634 (5)	6.8 (2)
C(75)	0.2450 (2)	0.8925 (3)	−0.4132 (5)	6.2 (2)
C(76)	0.2399 (2)	0.8388 (3)	−0.3283 (5)	5.2 (2)
C(81)	0.2431 (3)	0.7617 (2)	−0.0726 (5)	4.3 (2)
C(82)	0.2838 (3)	0.7066 (2)	−0.0388 (5)	6.3 (2)
C(83)	0.3548 (3)	0.7366 (2)	0.0585 (5)	9.1 (3)
C(84)	0.3852 (3)	0.8219 (2)	0.1221 (5)	9.3 (3)
C(85)	0.3445 (3)	0.8770 (2)	0.0883 (5)	8.1 (3)
C(86)	0.2734 (3)	0.8469 (2)	−0.0090 (5)	6.3 (2)

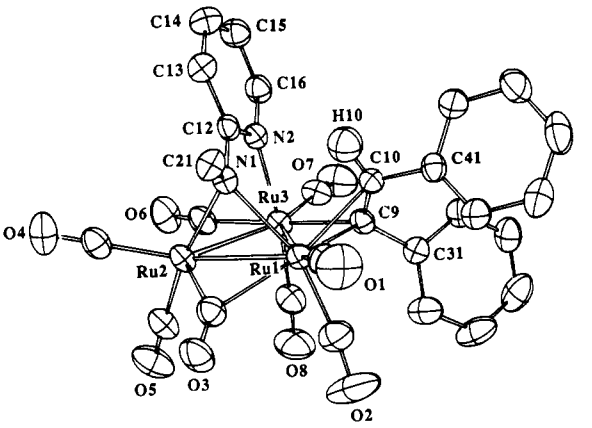

Figure 3. Perspective view of the alkenyl complex $Ru_3(\mu_3\text{-}\eta^2\text{-}N(C_6H_5)(C_5H_4N))(\mu\text{-}\eta^2\text{-}(C_6H_5)CCH(C_6H_5))(CO)_8$ (**4a**). The phenyl ring of the phenylpyridylamido group has been omitted for clarity. Thermal ellipsoids are shown at 30% probability level.

minutes with phosphines. In our hands, the substitution reactions involving diphenylphosphine proceeded within 2 min at temperatures as low as −30 °C.[9]

Interestingly, **3a,b** were found to react cleanly with diphenylacetylene under rather mild conditions (40–50 °C, 30 min) to give exclusively the new alkenyl species $Ru_3(\mu_3\text{-}\eta^2\text{-}X(C_5H_4N))((\mu\text{-}(C_6H_5)CCH(C_6H_5))(CO)_8$ (**4a,b**) (**4a**, 90–95% yield; **4b**, 70–80% yield) via cis insertion into the ruthenium–hydride bond. This reaction illustrates the ability of the hemilabile ancillary ligands $N(C_6H_5)(C_5H_4N)$ and $S(C_5H_4N)$ to preserve the trimetallic framework. Indeed, although the edge double-bridged complexes involving bridging halides or acyl groups readily incorporate alkynes or olefins via multiple insertion reactions which are of high interest,[30] subsequent loss of one metal center easily takes place to give bimetallic complexes.[28b,30] Such a degradation is avoided in **3a,b** by coordination of the pyridyl group to the third metal center. Huttner and co-workers have recently observed a similar stabilizing effect ascribed to a face-bridging thiolato group in the iron complex $Fe_3(\mu\text{-}H)(\mu_3\text{-}S^tBu)(CO)_9$ which also reacts with diphenylacetylene upon photochemical activation to give the alkenyl derivative $Fe_3(\mu\text{-}\eta^2(C_6H_5)CCH(C_6H_5))(\mu_3\text{-}S^tBu)(CO)_8$.[31]

F. Structure of the Alkenyl Complex $Ru_3(\mu\text{-}\eta^2\text{-}N(C_6H_5)(C_5H_4N))(\mu\text{-}(C_6H_5)CCH(C_6H_5))(CO)_8$ (4a). The structure of $Ru_3(\mu_3\text{-}\eta^2\text{-}N(C_6H_5)(C_5H_4N))(\mu\text{-}(C_6H_5)CCH(C_6H_5))(CO)_8$ (**4a**), determined by X-ray crystallography, is shown in Figure 3. It consists of a closed triruthenium unit supported by a face-bridging phenylpyridylamido group as referred to the structure of the antecedent complex **3a**.[10] The metal–metal edge Ru(1)–Ru(2), which is doubly bridged by the amido group and a carbonyl ligand, is significantly shorter than the two others (Ru(1)–Ru(2) = 2.6786 (3) Å; Ru(1)–Ru(3) = 2.8044 (4) Å; Ru(2)–Ru(3) = 2.8198 (5) Å). The alkenyl group spans the metal–metal edge Ru(1)–Ru(3), with the α-carbon occupying equatorial coordination sites and the β-carbon being linked to Ru(1) in a cis position relative to the nitrogen atom of the amido group. The structural features of this alkenyl group com-

(30) (a) Xue, Z.; Sieber, W. J.; Knobler, C. B.; Kaesz, H. D. *J. Am. Chem. Soc.* **1990**, *112*, 1825–1833 and references therein. (b) Boag, N. M.; Sieber, W. J.; Kampe, C. E.; Knobler, C. B.; Kaesz, H. D. *J. Organomet. Chem.* **1988**, *355*, 385–400.

(31) Fässler. T.; Huttner, G. *J. Organomet. Chem.* **1989**, *376*, 367–384.

Table VI. Selected Interatomic Distances (Å) for PPN•2a with Esd's in Parentheses[a]

		Ru–Ru			
		Ru(1)–Ru(2)	2.668 (1)		
Ru(1)–Ru(3)	2.783 (1)			Ru(2)–Ru(3)	2.795 (1)
		Ru–C (Terminal Carbonyl Groups in Equatorial Position)			
Ru(1)–C(1)	1.873 (9)			Ru(2)–C(4)	1.889 (8)
		Ru(3)–C(7)	1.875 (7)		
		Ru–C (Terminal Carbonyl Groups in Axial Position)			
Ru(1)–C(2)	1.842 (8)			Ru(2)–C(5)	1.860 (9)
		Ru(3)–C(8)	1.861 (8)		
		Ru–C (Bridging Carbonyl Groups in Equatorial Position)			
Ru(1)–C(3)	2.143 (8)			Ru(2)–C(3)	2.116 (7)
Ru(1)–C(9)	2.138 (7)			Ru(2)–C(6)	2.117 (6)
Ru(3)–C(9)	2.110 (9)			Ru(3)–C(6)	2.101 (9)
		Ru–N (from 2-Anilinopyridyl Ligand)			
Ru(1)–N(1)	2.237 (5)			Ru(2)–N(1)	2.246 (6)
		Ru(3)–N(2)	2.159 (6)		
		2-Anilinopyridyl Ligand[a]			
N(1)–C(12)	1.398 (8)	C(12)–N(2)	1.344 (7)	C(12)–C(13)	1.41 (1)
C(13)–C(14)	1.37 (1)	C(14)–C(15)	1.38 (1)	C(15)–C(16)	1.36 (1)
C(16)–N(2)	1.353 (8)	N(1)–C(21)	1.459 (6)		
		C–O (Terminal Carbonyl Groups in Equatorial Position)			
C(1)–O(1)	1.15 (1)			C(4)–O(4)	1.14 (1)
		C(7)–O(7)	1.145 (9)		
		C–O (Terminal Carbonyl Groups in Axial Position)			
C(2)–O(2)	1.15 (1)			C(5)–O(5)	1.14 (1)
		C(8)–O(8)	1.14 (1)		
		C–O (Bridging Carbonyl Groups in Equatorial Position)			
		C(3)–O(3)	1.157 (8)		
C(9)–O(9)	1.15 (1)			C(6)–O(6)	1.16 (1)
		Bis(triphenylphosphoranylidene)ammonium Cation, PPN^+			
P(1)–N(3)	1.573 (6)			P(2)–N(3)	1.589 (6)
P(1)–C(31)	1.793 (6)			P(2)–C(61)	1.790 (5)
P(1)–C(41)	1.783 (5)			P(2)–C(71)	1.790 (6)
P(1)–C(51)	1.789 (4)			P(2)–C(81)	1.790 (6)

[a] All phenyl rings treated as rigid groups: C–C = 1.395 Å, C–H = 0.97 Å.

pare well with those found in binuclear[30,32] or trinuclear[31,33] alkenyl complexes of the iron triad.

Discussion

The equilibrium between the decacarbonyl derivative PPN·1 and the corresponding nonacarbonyl species PPN·2 (eq 2, vide infra) is seen to parallel the equilibrium between $PPN[Ru_3(Cl)(CO)_{11}]$ and $PPN[Ru_3(\mu\text{-}Cl))(CO)_{10}]$ (eq 1, vide supra).

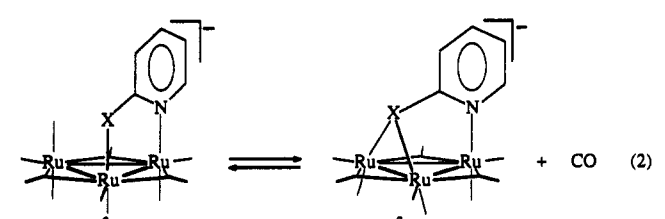

$[Ru_3(\mu\text{-}\eta^2\text{-}Xpy)(CO)_{10}]^-$ (1) $[Ru_3(\mu_3\eta^2\text{-}Xpy)(CO)_9]^-$ (2)

Whereas the activity and selectivity of mononuclear homogeneous catalysts are generally well controlled by a wide variety of phosphines,[34] these are not always the best choices as ancillary ligands for metal carbonyl clusters.[6c] Indeed, a recurrent difficulty in tailoring metastable polymetallic complexes in view of catalytic applications[35] is to reach the appropriate balance between the reactivity of the metal ensemble and its stability. Retention of a polymetallic framework may be effective when strongly coordinated polydentate phosphines are used as ancillary

(32) For leading references on binuclear alkenyl complexes of the iron triad, see: (a) Dyke, A. F.; Knox, S. A. R.; Morris, M. J.; Naish, P. J. *J. Chem. Soc., Dalton Trans.* **1983**, 1417. (b) Fildes, M. J.; Knox, S. A. R.; Orpen, G.; Turner, M. L.; Yates, M. I. *J. Chem. Soc., Chem. Commun.* **1989**, 1680–1682. (c) Bruce, G. C.; Knox, S. A. R.; Phillips, A. J. *J. Chem. Soc., Chem. Commun.* **1990**, 716–718. (d) Bruce, G. C. Gangnus, B.; Garner, S. E.; Knox, S. A. R.; Orpen, A. G.; Phillips, A. J. *J. Chem. Soc., Chem. Commun.* **1990**, 1360–1362. (e) Knox, S. A. R. *J. Organomet. Chem.* **1990**, *400*, 255–272, and references therein. (f) Yanez, R.; Ros, J.; Dahan, F.; Mathieu, R. *Organometallics* **1990**, *9*, 2484–2488. (g) Suzuki, H.; Omori, H.; Moro-Oka, Y. *Organometallics* **1988**, *7*, 2579–2581.

(33) For leading references on trinuclear alkenyl complexes of the iron triad, see: (a) Deeming, A. J.; Hasso, S.; Underhill, M. *J. Chem. Soc., Dalton Trans.* **1975**, 1614–1620. (b) Keister, J. B.; Shapley, J. R. *J. Organomet. Chem.* **1975**, *85*, C29-C31. (c) Guy, J. J.; Reichert, B. E.; Sheldrick, G. M. *Acta Crystallogr.* **1976**, B32, 3319–3320. (d) Orpen, A. G.; Pippard, D.; Sheldrick, G. M.; Rouse, K. D. *Acta Crystallogr.* **1978**, B34, 2466–2472. (e) Sappa, E.; Tiripicchio, A.; Manotti Lanfredi, A. M. *J. Organomet. Chem.* **1983**, *249*, 391–404. (f) Chi, Y.; Chen, B.-F.; Wang, S.-L.; Chiang, R.-K.; Hwang, L.-S. *J. Organomet. Chem.* **1989**, *377*, C59-C64. (g) Adams, R. D.; Chen, G.; Tanner, J. T. *Organometallics* **1990**, *9*, 1530–1538. (h) Chuang, S.-H.; Chi, Y.; Liao, F.-L.; Wang, S.-L.; Peng, S.-M.; Lee, G.-H.; Wu, J.-C.; Horng, K.-M. *J. Organomet. Chem.* **1991**, *410*, 85–99.

(34) (a) Collman, J. P.; Hegedus, S. *Principles and Applications of Organotransition Metal Chemistry*; University Science Books: Mill Valley, CA, 1980. (b) Wilkinson, G., Stone, F. G. A., Abel, E. W., Eds. *Comprehensive Organometallic Chemistry*; Pergamon Press: Oxford, 1982. (c) Yamamoto, A. *Organotransition Metal Chemistry*; Wiley: New York, 1986.

(35) For recent reviews on the applications of clusters as homogeneous catalysts, see: (a) Süss-Fink, G.; Neumann, F. *The Chemistry of Metal-Carbon Bonds*; Hartley, F. R., Ed.: Wiley: New York, 1989; Vol. 5, pp 231–317. (b) Gladfelter, W. L.; Roesselet, K. J. In *The Chemistry of Metal Clusters*; Shriver, D.; Adams, R. D.; Kaesz, H. D., Eds.; Verlag Chemie: Weinheim, 1990; Chapter 7, pp 329–365 and references therein.

Table VII. Selected Bond Angles (deg) for PPN•2a with Esd's in Parentheses

		Ru–Ru–Ru			
		Ru(1)–Ru(3)–Ru(2)	57.14 (2)		
Ru(2)–Ru(1)–Ru(3)	61.64 (2)			Ru(1)–Ru(2)–Ru(3)	61.21 (2)
		Ru–Ru–N (Anilinopyridyl Group)			
Ru(2)–Ru(1)–N(1)	53.6 (1)			Ru(1)–Ru(2)–N(1)	53.3 (1)
Ru(3)–Ru(1)–N(1)	75.8 (1)			Ru(3)–Ru(2)–N(1)	75.5 (1)
Ru(1)–Ru(3)–N(2)	85.0 (1)			Ru(2)–Ru(3)–N(2)	84.1 (1)
		Ru–Ru–CO (Axial Carbonyls)			
Ru(3)–Ru(1)–C(2)	100.1 (2)			Ru(3)–Ru(2)–C(5)	99.0 (2)
Ru(2)–Ru(1)–C(2)	112.9 (3)			Ru(1)–Ru(2)–C(5)	110.4 (3)
Ru(1)–Ru(3)–C(8)	93.1 (2)			Ru(2)–Ru(3)–C(8)	94.0 (3)
		N–Ru–CO			
N(1)–Ru(1)–C(1)	104.1 (3)			N(1)–Ru(2)–C(4)	103.8 (3)
N(1)–Ru(1)–C(2)	166.3 (3)			N(1)–Ru(2)–C(5)	163.6 (3)
N(1)–Ru(1)–C(3)	78.5 (2)			N(1)–Ru(2)–C(3)	78.9 (2)
N(1)–Ru(1)–C(9)	100.0 (2)			N(1)–Ru(2)–C(6)	101.1 (2)
N(2)–Ru(3)–C(9)	84.7 (3)			N(2)–Ru(3)–C(6)	84.4 (3)
		N(2)–Ru(3)–C(7)	94.4 (3)		
		N(2)–Ru(3)–C(8)	177.8 (2)		
		CO–Ru–CO (Adjacent Carbonyl Ligands Only)			
C(1)–Ru(1)–C(2)	86.9 (4)			C(4)–Ru(2)–C(5)	90.3 (4)
C(3)–Ru(1)–C(2)	90.9 (3)			C(3)–Ru(2)–C(5)	88.9 (3)
C(9)–Ru(1)–C(2)	86.4 (3)			C(6)–Ru(2)–C(5)	85.7 (3)
C(9)–Ru(3)–C(7)	108.5 (3)			C(6)–Ru(3)–C(7)	96.1 (3)
C(9)–Ru(3)–C(8)	94.9 (4)			C(6)–Ru(3)–C(8)	95.1 (4)
C(1)–Ru(1)–C(3)	105.3 (3)			C(4)–Ru(2)–C(3)	108.1 (3)
C(1)–Ru(1)–C(9)	97.1 (3)			C(4)–Ru(2)–C(6)	94.8 (3)
		C(7)–Ru(3)–C(8)	87.8 (3)		
C(7)–Ru(3)–C(9)	108.5 (3)			C(7)–Ru(3)–C(6)	96.1 (3)
C(8)–Ru(3)–C(9)	94.9 (4)			C(8)–Ru(3)–C(6)	95.1 (4)
		Ru–C–O (Terminal Carbonyl Ligands in Equatorial Position)			
Ru(1)–C(1)–O(1)	175.1 (8)			Ru(2)–C(4)–O(4)	176.2 (7)
		Ru(3)–C(7)–O(7)	173.4 (9)		
		Ru–C–O (Terminal Carbonyl Ligands in Axial Position)			
Ru(1)–C(2)–O(2)	175.2 (7)			Ru(2)–C(5)–O(5)	177.8 (7)
		Ru(3)–C(8)–O(8)	179.6 (7)		
		Ru–C–O (Bridging Carbonyl Ligands in Equatorial Position)			
Ru(1)–C(3)–O(3)	140.1 (7)			Ru(2)–C(3)–O(3)	141.3 (7)
Ru(1)–C(9)–O(9)	135.5 (5)			Ru(2)–C(6)–O(6)	137.4 (6)
Ru(3)–C(9)–O(9)	142.5 (5)			Ru(3)–C(6)–O(6)	139.4 (5)
		Anilinopyridyl Group (Intramolecular Angles)			
N(1)–C(12)–N(2)	116.9 (5)			N(1)–C(12)–C(13)	122.8 (5)
N(2)–C(12)–C(13)	120.2 (5)			N(2)–C(16)–C(15)	123.7 (6)
C(12)–C(13)–C(14)	119.8 (6)			C(14)–C(15)–C(16)	118.7 (7)
C(12)–N(2)–C(16)	118.3 (6)			C(13)–C(14)–C(15)	119.1 (8)
		Bis(triphenylphosphoranylidene)ammonium Cation, PPN^+			
		P(1)–N(3)–P(2)	136.8 (4)		

ligands. Unfortunately, such a stabilization may occur at the expense of reactivity. Furthermore, the cluster-assisted degradation of phosphine ligands is a facile process,[6c] and its relevance to homogeneous catalyst deactivation has been stressed.[36]

On the other hand, anionic nucleophiles such as halides or pseudo-halides are interesting ancillary ligands to consider in account of their cis-labilizing properties; yet, their applications to homogeneous systems effectively based on metal clusters may be restricted to very mild and specific conditions.[4]

In this context, the hybrid ancillary ligands used in this work may be classified as "hemilabile", in that they function as moderately stabilizing ligands possessing a lightly coordinated nucleophilic group (also working as a CO labilizer). Among the three ligands considered here, the phenylpyridylamido and pyridinethiolato groups are likely the most attractive ones. The pyridylalkoxo ligand is of more limited use here since we have seen that acidification of the corresponding anionic complex leads to the formation of $Ru_3(CO)_{12}$, probably via protonation at the oxygen atom.

The very mild conditions under which the interconversion between the anionic species **1a** and **2a** takes place (see eq 2) indicate that the reversible opening of an amido bridge is a low activation energy process. Though such a bridge opening is not observed when any of the neutral hydrido complexes **3a,b** is treated with CO, intermediates involving terminal amido or thiolato groups have been observed in the case of osmium.[24,25,27] Thus, one may reasonably suggest that opening of amido or thiolato bridges within the neutral hydrido complexes **3a,b** occurs as a transition state permitting the incorporation of an alkyne into the ligand shell of the cluster. Further elementary steps likely involve alkyne insertion into the metal–hydride bond and closure of the amido or mercapto

(36) Garrou, P. E. *Chem. Rev.* **1985**, *85*, 171.

bridge with concomitant loss of a carbonyl group to provide the alkenyl species **4a,b** (eq 3).

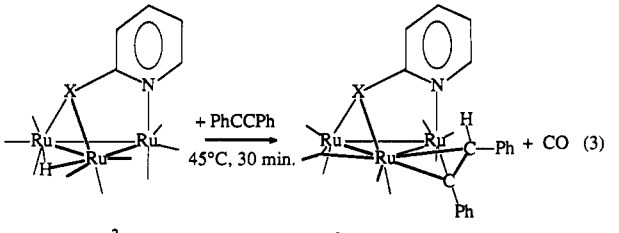

$Ru_3(\mu\text{-}H)(\mu_3\,\eta^2\text{-}Xpy)(CO)_9$ (3) $Ru_3(\mu_3\,\eta^2\text{-}Xpy)(\mu\text{-}PhCCHPh)(CO)_8$ (4)

Such a reaction sequence highlights an important advantage of these "lightly ligand-bridged" cluster systems with respect to electronically unsaturated species: Obviously, any electronically unsaturated 46-electron cluster complex will saturate by incorporation of just one ligand donating 2 electrons, thereby becoming much less susceptible to react further with weakly nucleophilic incoming substrates. By contrast, a vacant site may still become available within the species **4a,b** via the repeated bridge-opening sequence described above. Such a process may account for the facile addition of ethylene to **4a**, permitting its subsequent coupling with the alkenyl group to give a butadiene,[9] a reaction that remains rare for polynuclear[32c,d] and mononuclear[37] complexes.

While we are reporting part of our work in the present paper, we have now observed new coupling reactions involving the alkenyl group of complex **4a** and other organic substrates such as alkynes and isonitriles.[38] Studies aimed to determine the mechanism of carbon–carbon coupling reactions involving the reactive alkenyl complex reported here are under way.

Experimental Section

General Comments. All synthetic manipulations were carried out under nitrogen atmosphere, using standard Schlenk techniques. Tetrahydrofuran was distilled under argon from sodium benzophenone ketyl just before use. Dichloromethane and benzene were purified following standard procedures and stored under nitrogen. The following reagent-grade chemicals, bis(triphenylphosphoranylidene)ammonium chloride ((PPN)Cl), K-Selectride, 2-anilinopyridine, 2-hydroxypyridine, 2-mercaptopyridine, were obtained from Aldrich. The reagent 2-anilinopyridine was sublimed prior to use. The following starting materials were prepared according to published procedures: $Ru_3(CO)_{12}$;[39] (PPN)BH_4;[40] PPN[$HRu_3(CO)_{11}$].[17e]

Infrared spectra were recorded on a Perkin-Elmer 225 spectrophotometer with 0.1-mm cells equipped with CaF_2 windows. These spectra were calibrated against water vapor absorptions. ^1H, ^{31}P, and ^{13}C NMR spectra were obtained on Bruker WH90, AC80, or AC200 spectrometers. Chromatographic separation of type 3 complexes was carried out on silica gel columns (Kieselgel 60 (Merck), 70–230-mesh ASTM).

Each of the three preparative methods mentioned in the text is detailed below in one typical example: method i for 2-mercaptopyridine derivatives, method ii for 2-hydroxypyridine derivatives, and method iii for 2-anilinopyridine derivatives.

In Situ Formation of PPN[$Ru_3(\mu\text{-}\eta^2\text{-}N(C_6H_5)(C_5H_4N))(CO)_{10}$] (PPN·1a). This complex is quantitatively obtained in situ when CO gas is bubbled for 5–10 min into THF solutions of PPN·**2a** (vide infra) at 25 °C; its formation can be monitored by infrared spectroscopy.

PPN·**1a**: IR (ν(CO), cm^{-1}, THF) 2066 m, 2035 vw, 2007 vs, 1985 vs, 1951 m, 1935 m, 1925 sh, 1855 vw, 1811–1800 s, br.

Preparation of PPN[$Ru_3(\mu\text{-}\eta^2\text{-}O(C_5H_4N))(CO)_{10}$] (PPN·1c). Method i. In a typical experiment, 60 mg (0.625 mmol) of freshly sublimed 2-hydroxypyridine was added to a suspension of 20 mg of NaH powder in 10 mL of THF. When the gaseous evolution stopped, the suspension of the resulting salt was added to a solution containing 400 mg (0.625 mmol) of $Ru_3(CO)_{12}$ in 40 mL of THF. The solution was then heated under reflux for 45 min. The sodium salt Na·**1c** obtained in solution was found to exhibit the following IR absorption bands: 2069 w, 2055 vw, 2012 vs, 1985 s, 1953 m, 1936 ms, 1859 vw, 1814–1803 cm^{-1} s, br. After cooling and evaporation of the solvent, the residue was dissolved in 20 mL of dry ethanol. A stoichiometric amount of (PPN)Cl was added (360 mg, 0.625 mmol), and the solution was refrigerated. After a few minutes at −30 °C, abundant precipitation of the complex was observed. About 500 mg of the complex PPN-[$Ru_3(\mu\text{-}O(C_5H_4N))(CO)_{10}$] (PPN·1c) was separated by filtration (65% yield).

Table VIII. Fractional Atomic Coordinates and Isotropic or Equivalent Temperature Factors (Å² × 100) for 4a with Esd's in Parentheses

atom	x/a	y/b	z/c	U_{eq}/U_{iso}
Ru(1)	0.88273 (2)	0.78059 (1)	0.36326 (3)	2.85 (4)
Ru(2)	0.95770 (3)	0.64189 (1)	0.28083 (3)	3.21 (4)
Ru(3)	1.04197 (2)	0.68385 (1)	0.59382 (3)	2.90 (4)
N(1)	0.7662 (3)	0.6905 (1)	0.3406 (3)	3.0 (4)
N(2)	0.8530 (3)	0.6533 (1)	0.5968 (3)	3.1 (4)
C(12)	0.7505 (3)	0.6570 (2)	0.4679 (3)	3.0 (5)
C(13)	0.6372 (3)	0.6265 (2)	0.4628 (4)	4.2 (6)
C(14)	0.6296 (4)	0.5930 (2)	0.5897 (5)	5.2 (7)
C(15)	0.7329 (4)	0.5905 (2)	0.7227 (4)	5.0 (6)
C(16)	0.8417 (4)	0.6205 (2)	0.7222 (4)	4.0 (5)
C(1)	0.7419 (4)	0.8496 (2)	0.2394 (4)	4.1 (6)
O(1)	0.6653 (3)	0.8913 (2)	0.1619 (4)	6.4 (6)
C(2)	0.9983 (4)	0.8373 (2)	0.3298 (4)	5.3 (7)
O(2)	1.0641 (4)	0.8702 (2)	0.2900 (4)	10.5 (8)
C(3)	0.9139 (3)	0.7258 (2)	0.1471 (4)	3.9 (5)
O(3)	0.9085 (3)	0.7448 (1)	0.0240 (3)	5.7 (5)
C(4)	0.9089 (4)	0.5617 (2)	0.1584 (4)	4.3 (6)
O(4)	0.8815 (3)	0.5115 (2)	0.0862 (3)	6.4 (6)
C(5)	1.1322 (4)	0.6132 (2)	0.2555 (4)	4.5 (6)
O(5)	1.2409 (3)	0.5954 (2)	0.2443 (4)	7.0 (6)
C(6)	1.1007 (4)	0.5792 (2)	0.5526 (4)	4.1 (6)
O(6)	1.1427 (3)	0.5185 (1)	0.5577 (3)	5.8 (5)
C(7)	1.1168 (3)	0.6743 (2)	0.8154 (4)	4.2 (6)
O(7)	1.1692 (3)	0.6701 (2)	0.9418 (3)	6.9 (6)
C(8)	1.2021 (3)	0.7047 (2)	0.5646 (4)	4.5 (6)
O(8)	1.3016 (3)	0.7134 (2)	0.5457 (4)	7.9 (7)
C(9)	0.9602 (3)	0.7947 (2)	0.6235 (3)	3.2 (5)
C(10)	0.8198 (3)	0.8168 (2)	0.5892 (4)	3.2 (5)
C(21)	0.6393 (3)	0.7121 (2)	0.2240 (4)	3.4 (5)
C(22)	0.5321 (4)	0.7584 (2)	0.2654 (4)	4.4 (6)
C(23)	0.4137 (4)	0.7834 (2)	0.1549 (6)	5.4 (7)
C(24)	0.4021 (4)	0.7637 (2)	0.0024 (5)	5.8 (8)
C(25)	0.5075 (5)	0.7181 (2)	−0.0400 (5)	5.8 (8)
C(26)	0.6251 (4)	0.6908 (2)	0.0710 (4)	4.6 (6)
C(31)	1.0459 (3)	0.8463 (2)	0.7113 (4)	3.3 (5)
C(32)	1.0257 (4)	0.8707 (2)	0.8565 (4)	4.0 (5)
C(33)	1.1008 (4)	0.9180 (2)	0.9465 (4)	4.8 (6)
C(34)	1.1938 (5)	0.9445 (2)	0.8952 (5)	6.0 (8)
C(35)	1.2177 (5)	0.9208 (3)	0.7548 (5)	6.8 (8)
C(36)	1.1455 (4)	0.8711 (2)	0.6649 (4)	5.3 (7)
C(41)	0.7449 (3)	0.8904 (2)	0.6192 (4)	3.2 (5)
C(42)	0.7703 (4)	0.9546 (2)	0.5764 (4)	4.4 (6)
C(43)	0.7011 (4)	1.0208 (2)	0.6155 (5)	5.1 (7)
C(44)	0.6044 (4)	1.0241 (2)	0.6957 (5)	5.5 (7)
C(45)	0.5785 (4)	0.9614 (2)	0.7398 (5)	5.9 (7)
C(46)	0.6466 (4)	0.8945 (2)	0.6998 (5)	4.9 (6)
H(10)	0.763 (4)	0.782 (2)	0.589 (5)	6.00 (0)
	Dichloromethane Molecule (Disordered)			
Cl	0.5571 (2)	0.4796 (1)	0.1618 (2)	13.2 (5)
C	0.555 (1)	0.4660 (7)	0.978 (2)	10 (3)

(37) (a) Herrmann, W. A.; Fischer, R. A.; Herdtweck, E. *Organometallics* **1989**, *8*, 2821–2831. (b) Salerno, G.; Panza, M.; Chiusoli, G. P.; Costa, M. *J. Organomet. Chem.* **1990**, *394*, 569–581. (c) Mitsudo, T.; Zhang, S.-W.; Nagao, M.; Watanabe, Y. *J. Chem. Soc., Chem. Commun.* **1991**, 598–599.

(38) Mulla, F.; Lugan, N.; Lavigne, G.; Bonnet, J.-J. In preparation.

(39) Mantovani, A.; Cenini, S. *Inorg. Synth.* **1972**, *16*, 47–48.

(40) Kirtley, S. W.; Andrews, M. A.; Bau, R.; Grynkewich, G. W.; Marks, T. J.; Tipton, D. L.; Whittlesey, B. R. *J. Am. Chem. Soc.* **1977**, *99*, 7154–7162.

Table IX. Selected Interatomic Distances (Å) for 4a with Esd's in Parentheses

		Ru–Ru			
		Ru(1)–Ru(2)	2.6786 (3)		
Ru(1)–Ru(3)	2.8044 (4)			Ru(2)–Ru(3)	2.8198 (5)
		Ru–C (Terminal Carbonyl Groups in Equatorial Position)			
Ru(1)–C(1)	1.914 (3)			Ru(2)–C(4)	1.877 (4)
		Ru(3)–C(7)	1.942 (3)	Ru(3)–C(6)	1.979 (3)
Ru(1)–C(2)	1.850 (5)			Ru(2)–C(5)	1.860 (4)
		Ru(3)–C(8)	1.874 (4)		
		Ru–C (Bridging Carbonyl Group in Equatorial Position)			
Ru(1)–C(3)	2.199 (4)			Ru(2)–C(3)	1.956 (4)
		Ru–N (from 2-Anilinopyridyl Ligand)			
Ru(1)–N(1)	2.242 (3)			Ru(2)–N(1)	2.207 (3)
		Ru(3)–N(2)	2.166 (3)		
		Ru–C (Alkenyl Group)			
Ru(1)–C(9)	2.276 (3)	Ru(3)–C(9)	2.114 (3)	Ru(1)–C(10)	2.306 (3)
		2-Anilinopyridyl Ligand			
N(1)–C(12)	1.401 (4)	C(12)–N(2)	1.349 (3)	C(12)–C(13)	1.402 (5)
C(13)–C(14)	1.364 (6)	C(14)–C(15)	1.380 (5)	C(15)–C(16)	1.364 (6)
C(16)–N(2)	1.361 (5)	N(1)–C(21)	1.460 (3)	C(21)–C(22)	1.389 (5)
C(22)–C(23)	1.386 (5)	C(23)–C(24)	1.372 (7)	C(24)–C(25)	1.372 (6)
C(25)–C(26)	1.394 (5)	C(26)–C(21)	1.380 (5)		
		Alkenyl Group			
C(9)–C(10)	1.397 (4)	C(10)–H(10)	0.97 (5)	C(9)–C(31)	1.495 (4)
C(10)–C(41)	1.491 (4)	C(31)–C(32)	1.403 (5)	C(32)–C(33)	1.380 (5)
C(33)–C(34)	1.362 (7)	C(34)–C(35)	1.374 (6)	C(35)–C(36)	1.395 (6)
C(36)–C(31)	1.383 (6)	C(41)–C(42)	1.384 (5)	C(42)–C(43)	1.380 (5)
C(43)–C(44)	1.373 (7)	C(44)–C(45)	1.364 (6)	C(45)–C(46)	1.389 (5)
C(46)–C(41)	1.387 (6)				
		C–O (Terminal Carbonyl Groups in Equatorial Position)			
C(1)–O(1)	1.128 (4)			C(4)–O(4)	1.147 95)
		C(7)–O(7)	1.123 (4)	C(6)–O(6)	1.138 (4)
		C–O (Terminal Carbonyl Groups in Axial Position)			
C(2)–O(2)	1.143 (7)			C(5)–O(5)	1.145 (5)
		C(8)–O(8)	1.138 (5)		
		C–O (Bridging Carbonyl Group in Equatorial Position)			
		C(3)–O(3)	1.168 (5)		

Method ii. In a typical experiment, a 60-mg sample of 2-hydroxypyridine (0.625 mmol) was added to a solution of PPN-[$Ru_3(\mu$-H)$(CO)_{11}$] prepared in situ[17e] from 400 mg of $Ru_3(CO)_{12}$ (0.625 mmol) and a stoichiometric amount of $(PPN)BH_4$ (350 mg, 0.625 mmol) in 40 mL of THF. The solution was then refluxed for 3 h during which the color changed from dark red to brown-yellow. The formation of the new complex was monitored by following the appearance of the strong ν(CO) absorption band at 1800 cm^{-1}. The THF was then evaporated under reduced pressure, and the complex was crystallized in 60–65% yield from acetone/ethanol mixtures.

PPN[$Ru_3(\mu$-O$(C_5H_4N))(CO)_{10}$] (PPN·**1c**): IR (ν(CO), cm^{-1}, THF) 2070 m, 2011 vs, 1986 vs, 1953 m, 1936 m, 1926 sh, 1856 vw, 1812–1802 s, br. Anal. Calcd for $C_{51}H_{34}N_2O_{11}P_2Ru_3$: C, 50.37; H, 2.82; N, 2.30. Found: C, 50.57; H, 2.60; N, 2.10.

Preparation of PPN[$Ru_3(\mu_3$-η^2-$(C_6H_5)N(C_5H_4N))(CO)_9$] (PPN·2a) via Deprotonation of Complex 3a. In a typical procedure, a 300-mg sample of the complex $Ru_3(\mu$-H$)(\mu_3$-η^2-$(C_6H_5)N(C_5H_4N))(CO)_9$ (**3a**) (0.41 mmol) (prepared according to the procedure detailed below) was dissolved in 20 mL of THF. The salt $(PPN)BH_4$ (229 mg, 0.41 mmol) was dissolved separately in the minimum amount of CH_2Cl_2 (ca. 1 mL) and the resultant mixture added dropwise to the stirred solution of **3a**. The solution immediately turned yellow-brown. After 10 min, it was filtered through Celite and evaporated to dryness to give a yellow powder that could be recrystallized from methanol in up to 85–95% yield. Suitable crystals for the X-ray diffraction analysis were grown from a mixture of dichloromethane and diethyl ether.

PPN·**2a**: IR (ν(CO), cm^{-1}, THF) 2021 s, 2012 sh, 1976 vs, 1934 ms, 1912 m, 1842 vw, 1793 vs. Anal. Calcd for $C_{56}H_{39}N_3O_9P_2Ru_3$: C, 53.25; H, 3.11; N, 3.33. Found: C, 53.36; H, 3.10; N, 3.36.

Preparation of PPN[$Ru_3(\mu_3$-η^2-S$(C_5H_4N))(CO)_9$] (PPN·2b). Method i. In a typical procedure, the salt $KS(C_5H_4N)$ was prepared in situ at 25 °C from a solution of 2-mercaptopyridine (90 mg) in 20 mL of THF by dropwise addition of a stoichiometric amount of K-Selectride (alternatively, *n*-butyllithium, KH, or NaH could be used for this reduction). The addition induced the precipitation of a white powder. The point of exact titration was indicated by the net disappearance of the yellow of 2-mercaptopyridine upon its quantitative conversion into the colorless salt $KS(C_5H_4N)$. A 500-mg sample of $Ru_3(CO)_{12}$ (0.78 mmol) was added directly into the Schlenk containing the suspension of $KS(C_5H_4N)$. Rapid dissolution of both $Ru_3(CO)_{12}$ and $KS(C_5H_4N)$ was then observed. The formation of K[$Ru_3(\mu_3$-η^2-S$(C_5H_4N))(CO)_9$] (K·**2b**) was found to be spectroscopically quantitative after few minutes by infrared monitoring. After evaporation of the solvent under reduced pressure, the residue was first washed with hexane and then dissolved in 40 mL of methanol. The resulting solution was filtered to remove possible traces of $Ru_3(CO)_{12}$. Metathesis of the salt was carried out by addition of 10 mL of a methanol solution in which a 450-mg sample of (PPN)Cl (0.78 mmol) had been previously dissolved. After a few minutes, yellow crystals appeared. Precipitation was found to be complete within 2 h at −30 °C. Bright yellow crystals of PPN·**2b** were separated by filtration and washed with hexane and cold methanol (ca. 80–90% yield).

PPN·**2b**: IR (ν(CO), cm^{-1}, THF) 2020 s, 1975 vs, 1933 m, 1909 m, 1842 w, 1798 s, 1762 w. Anal. Calcd for $C_{50}H_{34}N_2O_9S_1P_2Ru_3$: C, 49.88; H, 2.85; N, 2.33. Found: C, 50.19; H, 2.71; N, 2.29.

In Situ Formation of PPN[$Ru_3(\mu_3$-η^2-O$(C_5H_4N))(CO)_9$] (PPN·2c). This complex was spectroscopically detected in situ after prolonged reflux of a solution of PPN·**1c** in THF under a stream of inert gas.

PPN[$Ru_3(\mu$-O$(C_5H_4N))(CO)_9$] (PPN·**2c**): IR (ν(CO), cm^{-1}, THF) 2024 m, 2011 sh, 1978 vs, 1935 s, 1920 sh, 1800 s.

Preparation of $Ru_3(\mu$-H$)(\mu$-N$(C_6H_5)(C_5H_4N))(CO)_9$ (3a). Method iii. In a typical experiment, 500 mg of $Ru_3(CO)_{12}$ (0.78 mmol) and 140 mg of freshly sublimed 2-anilinopyridine (0.78

Table X. Selected Bond Angles (deg) for 4a with Esd's in Parentheses

		Ru–Ru–Ru			
		Ru(1)–Ru(3)–Ru(2)	56.88 (1)		
Ru(2)–Ru(1)–Ru(3)	61.85 (1)			Ru(1)–Ru(2)–Ru(3)	61.269 (8)
		Ru–Ru–N (Anilinopyridyl Group)			
Ru(2)–Ru(1)–N(1)	52.38 (6)			Ru(1)–Ru(2)–N(1)	53.59 (7)
Ru(3)–Ru(1)–N(1)	76.38 (5)			Ru(3)–Ru(2)–N(1)	76.57 (6)
Ru(1)–Ru(3)–N(2)	85.16 (6)			Ru(2)–Ru(3)–N(2)	80.80 (6)
		N–Ru–C (between Anilinopyridyl and Alkenyl Groups)			
N(1)–Ru(1)–C(10)	88.4 (1)			N(1)–Ru(1)–C(9)	103.4 (1)
N(2)–Ru(3)–C(9)	91.0 (1)				
		Linkage of the Alkenyl Group			
Ru(1)–C(9)–Ru(3)	79.3 (1)			Ru(1)–C(10)–C(41)	124.8 (2)
Ru(1)–C(10)–C(9)	71.1 (2)			Ru(1)–C(10)–H(10)	99 (2)
Ru(1)–C(9)–C(10)	73.4 (2)			Ru(3)–C(9)–C(10)	118.8 (2)
Ru(1)–C(9)–C(31)	128.9 (2)			Ru(3)–C(9)–C(31)	121.6 (2)
		Ru–Ru–CO (Axial Carbonyls)			
Ru(3)–Ru(1)–C(2)	105.1 (1)			Ru(3)–Ru(2)–C(5)	94.7 (1)
Ru(2)–Ru(1)–C(2)	111.1 (1)			Ru(1)–Ru(2)–C(5)	117.4 (1)
Ru(1)–Ru(3)–C(8)	91.8 (1)			Ru(2)–Ru(3)–C(8)	91.6 (1)
		Ru–Ru–CO (Equatorial Carbonyls)			
Ru(2)–Ru(3)–C(6)	66.12 (9)			Ru(1)–Ru(3)–C(6)	122.98 (9)
Ru(2)–Ru(3)–C(7)	158.9 (1)			Ru(1)–Ru(3)–C(7)	143.6 (1)
		Ru–Ru–CO (Bridging Carbonyl)			
Ru(2)–Ru(1)–C(3)	45.98 (9)			Ru(1)–Ru(2)–C(3)	54.0 (1)
		N–Ru–CO			
N(1)–Ru(1)–C(1)	97.3 (1)			N(1)–Ru(2)–C(4)	101.4 (1)
N(1)–Ru(1)–C(3)	77.8 (1)			N(1)–Ru(2)–C(3)	83.9 (1)
N(2)–Ru(3)–C(6)	84.5 (1)			N(2)–Ru(3)–C(7)	94.2 (1)
		CO–Ru–CO (Adjacent Carbonyl Ligands Only)			
C(1)–Ru(1)–C(2)	85.3 (2)			C(4)–Ru(2)–C(5)	88.8 (2)
C(1)–Ru(1)–C(3)	87.6 (1)			C(4)–Ru(2)–C(3)	108.2 (1)
C(2)–Ru(1)–C(3)	83.6 (2)			C(5)–Ru(2)–C(3)	94.2 (2)
C(6)–Ru(3)–C(7)	93.1 (1)			C(6)–Ru(3)–C(8)	91.3 (2)
C(7)–Ru(3)–C(8)	92.4 (1)				
		Ru–C–O (Terminal Carbonyl Ligands in Equatorial Position)			
Ru(1)–C(1)–O(1)	175.3 (4)			Ru(2)–C(4)–O(4)	178.3 (3)
		Ru(3)–C(7)–O(7)	174.5 (4)	Ru(3)–C(6)–O(6)	167.4 (3)
		Ru–C–O (Terminal Carbonyl Ligands in Axial Position)			
Ru(1)–C(2)–O(2)	171.4 (3)			Ru(2)–C(5)–O(5)	178.1 (3)
		Ru(3)–C(8)–O(8)	176.2 (3)		
		Ru–C–O (Bridging Carbonyl Ligand in Equatorial Position)			
Ru(1)–C(3)–O(3)	135.2 (3)			Ru(2)–C(3)–O(3)	144.6 (3)
		2-Anilinopyridyl (Intramolecular Angles)			
Ru(1)–N(1)–C(12)	123.1 (2)			Ru(2)–N(1)–C(12)	111.8 (2)
Ru(1)–N(1)–C(21)	107.1 (2)			Ru(2)–N(1)–C(21)	122.7 (2)
Ru(3)–N(2)–C(12)	120.8 (2)			Ru(3)–N(2)–C(16)	120.5 (2)
C(12)–N(1)–C(21)	113.3 (3)			N(1)–C(12)–N(2)	116.5 (3)
N(1)–C(12)–C(13)	122.7 (2)				

mmol) were dissolved in 60 mL of benzene. The solution was then heated under reflux at 80 °C in an inert atmosphere. The initial orange gradually turned red-orange. IR monitoring showed the reaction to be complete within 2.5 h. After cooling, benzene was evacuated under reduced pressure and the solid residue was purified on a silica gel column. Elution with pure heptane was first carried out to eliminate traces of unreacted $Ru_3(CO)_{12}$. Further elution with a dichloromethane/heptane (1:3) mixture gave an orange band containing the new complex **3a**, which was subsequently recrystallized from dichloromethane/pentane (480 mg, 85% yield).

3a: orange crystals; IR (ν(CO), cm^{-1}, cyclohexane) 2078 m, 2050 vs, 2030 vs, 2000 s, 1993 m, 1971 w, 1966 w; ^1H NMR ($CDCl_3$, 298 K) δ −11.20 (s, μ-H). Anal. Calcd for $C_{20}H_{10}O_9N_2Ru_3$: C, 33.11; H, 1.39; N, 3.86. Found: C, 32.87; H, 1.39; N, 4.03.

Preparation of $Ru_3(\mu\text{-}H)(\mu\text{-}S(C_5H_4N))(CO)_9$ (3b). From K·2b, via Method i. In a typical procedure, the anion K·**2b** was prepared in situ as detailed above from 90 mg of 2-mercaptopyridine and 500 mg of $Ru_3(CO)_{12}$ in 40 mL of THF. The solution was then evaporated to dryness, and the solid residue was dissolved in 20 mL of dichloromethane. The anion was subsequently titrated by CF_3COOH at −20 °C. The resulting brown-yellow solution was finally evaporated to dryness, and the residue was purified on a silica gel column. The complex $Ru_3(\mu\text{-}H)(\mu_3\text{-}\eta^2\text{-}S\text{-}(C_5H_4N))(CO)_9$ (**3b**) eluted with a dichloromethane/hexane (1:4) mixture as an orange band. Recrystallization from dichloromethane/pentane mixtures afforded 400 mg of red-orange crystals (yield 81%).

Halide-Assisted Procedure. In a typical experiment, the complex $PPN[Ru_3(Cl)(CO)_{11}]$ was prepared in situ[3g,h] by addition of (PPN)Cl (180 mg, dissolved in 2 mL of dichloromethane) to a THF solution (20 mL) of $Ru_3(CO)_{12}$ (200 mg). A stoichiometric amount of 2-mercaptopyridine (40 mg) was added. IR monitoring indicated the rapid appearance of the characteristic CO absorption bands of complex **3b**, contaminated by those of the corresponding anion **2b** (easily identified by its characteristic strong μ-CO absorption band). The THF solvent was then evaporated to dryness and replaced by an equivalent volume of dichloromethane. The dichloromethane solution containing a mixture of **3b** and PPN·**2b** was subsequently titrated by CF_3COOH at −20 °C. After complete

disappearance of the μ-CO absorption of the anion, the solution was reduced in volume and purified by chromatography, leading to 150 mg of complex **3b** (70% yield).

3b: red-orange crystals; IR (ν(CO), cm^{-1}, cyclohexane) 2079 m, 2050 vs, 2030 vs, 2004 s, 1993 s, 1972 w, 1966 w; ^1H NMR ($CDCl_3$, 298 K) δ −13.15 (s, μ-H). Anal. Calcd for $C_{14}H_5O_9N_1S_1Ru_3$: C, 25.23; H, 0.76; N, 2.10. Found: C, 25.54; H, 0.79; N, 2.06.

Preparation of $Ru_3(\mu\text{-}H)(\mu\text{-}(C_6H_5)N(C_5H_4N))(\mu\text{-}(C_6H_5)CCH(C_6H_5))(CO)_8$ (4a). In a typical procedure, $Ru_3(\mu\text{-}H)(\mu_3\text{-}\eta^2\text{-}(C_6H_5)N(C_5H_4N))(CO)_9$ (**3a**) (325 mg) was dissolved in a mixture of dichloromethane (10 mL) and hexane (30 mL). A stoichiometric amount of diphenylacetylene (80 mg) was added, and the solution was heated at 45–50 °C under a slow nitrogen stream in a Schlenk flask equipped with a reflux condenser. The solution was initially orange and then turned purple and became progressively colorless as soon as a purple crystalline precipitate appeared on the glass walls of the flask. After 30–45 min, the solution was almost colorless, only containing traces of unreacted **3a**. After the mixture was cooled to room temperature, the deep red crystalline precipitate **4a**, almost insoluble in hexane, was filtered, washed with hexane, and dried under vacuum (371 mg, 94% yield). We noted that this complex could not be chromatographed since it was retained at the top of silica gel columns. Nevertheless, it could be easily purified by crystallization due to its poor solubility in hexane as compared with that of the antecedent complex **3a**. Crystals of **4a** suitable for X-ray diffraction were obtained by slow cooling of the mother liquor (dichloromethane/hexane). Unlike the powder samples obtained by rapid precipitation and used for the elemental analysis, the crystals were found to contain 1 mol of dichloromethane solvent per unit cell.

4a: red-violet powder; IR (ν(CO), cm^{-1}, THF) 2062 m, 2034 vs, 2007 vs, 1995 s, 1974 m, 1936 m, 1822 m; ^{13}C NMR ($CDCl_3$, 298 K) δ 75.0 (alkenyl carbon); ^1H NMR ($CDCl_3$, 298 K) δ 8.07–6.32 (aromatic protons). Anal. Calcd for $C_{33}H_{20}O_8N_2Ru_3$: C, 45.26; H, 2.30; N, 3.2. Found: C, 45.18; H, 2.17; N, 2.89.

$Ru_3(\mu\text{-}S(C_5H_4N))(\mu\text{-}(C_6H_5)CCH(C_6H_5))(CO)_8$ (4b). The complex **4b** (as well as its phenylacetylene analogue **4b**; vide infra) was prepared in a typical procedure analogous to that described for **4a** (see above), starting from 420 mg of **3b**. A 370-mg portion of crystals was then obtained (yield 71%).

4b: red-violet powder; IR (ν(CO), cm^{-1}, cyclohexane) 2066 m, 2042 vs, 2014 vs, 2001 m, 1986–1981 m, 1938 ms, 1810 m. Anal. Calcd for $C_{28}H_{17}O_8N_1S_1Ru_3Cl_2$: C, 37.3; H, 1.9; N, 1.55. Found: C, 37.57; H, 1.94; N, 1.64.

$Ru_3(\mu\text{-}S(C_5H_4N))(\mu\text{-}(C_6H_5)CCH_2)(CO)_8$ (4b′). The same preparative procedure as for **4a** was used; vide supra: yield 75%; red-violet powder; IR (ν(CO), cm^{-1}, THF) 2066 m, 2038 vs, 2008 vs, 1995 m, 1983 m, 1929 ms, 1797 m; ^1H NMR ($(CD_3)_2CO$, 298 K) δ 9.56–7.56 (aromatic protons), 4.23 (1 H, d, J_{H-H} = 2.35 Hz), 2.79 (1 H, d, J_{H-H} = 2.35 Hz). Anal. Calcd for $C_{21}H_{11}O_8N_1S_1Ru_3$: C, 34.06; H, 1.50; N, 1.89. Found: C, 34.13; H, 1.48; N, 1.61.

Crystal Data Collection and Reduction. Diffraction measurements were carried out on an Enraf-Nonius CAD4 diffractometer equipped with a graphite monochromator. Mo Kα radiation was used. The unit cells were determined and refined from the setting angles of 25 randomly selected reflections in the range 24° < 2θ (Mo $K\alpha_1$) < 28°. Crystal and intensity data for the compounds PPN·**1c**, PPN·**2a**, and **4a** are summarized in Table I. Data reductions were carried out using the SDP crystallographic computing package.[41] The intensities were corrected for absorption by using a numerical method based on GAUSSIAN integration[42] in the case of PPN·**1c** and **4a** and an empirical ψ-scan method in the case of PPN·**2a**.[41]

Solution and Refinement of the Structures. All calculations were performed on a MicroVAX 3400. The structures were solved by using the SHELXS package[43] and refined by using the SHELX-76 package.[44] The position of Ru atoms was determined by direct methods. All remaining non-hydrogen atoms were located by the usual combinations of full-matrix least-squares refinement and difference electron density syntheses. Atomic scattering factors were taken from the usual tabulations.[45] Anomalous dispersion terms for Ru and P atoms were included in F_c.[46] In order to reduce the large number of variable parameters in PPN·**1c** and PPN·**2a**, the phenyl groups of the bis(triphenylphosphine)iminium cations (PPN^+) were treated as rigid groups (imposed D_{6h} symmetry, with C–C = 1.395 Å and C–H = 0.97 Å). In all other cases, non-hydrogen atoms were allowed to vibrate anisotropically. The hydrogen atoms of phenyl and pyridyl groups were entered in idealized positions (C–H = 0.97 Å). Scattering factors for the hydrogen atoms were taken from Stewart et al.[47] Since the number of variables for **4a** was much lower than for the other structures, all non-hydrogen atoms of this complex were refined with anisotropic thermal parameters. The atomic coordinates of the hydrogen atom of the alkenyl group were also refined. Other hydrogen atoms of the latter complex were entered in idealized positions and were fixed in the final cycles of refinement. A disordered molecule of dichloromethane (solvent) was located in the lattice of **4a**, close to the inversion center. It could be correctly refined.

Figures and Tables of Results. Wherever possible, we have adopted the same labeling scheme for the three structures. Complex PPN·**1c**: An ORTEP diagram of the anionic unit is given in Figure 1. Final atomic coordinates and $U_{eq} \times 100$ (or $U_{iso} \times 100$) for all atoms are listed in Table II. Selected interatomic distances and interatomic bond angles of interest are given in Tables III and IV, respectively. Complex PPN·**2a**: A diagram of the anionic unit is given in Figure 2. Final atomic coordinates and $U_{eq} \times 100$ (or $U_{iso} \times 100$) are listed in Table V. Selected interatomic distances and interatomic bond angles of interest are given in Tables IV and VII, respectively. Complex **4a**: A diagram is given in Figure 3. Final atomic coordinates and $U_{eq} \times 100$ (or $U_{iso} \times 100$) are given in Table VIII. Selected interatomic distances and interatomic bond angles of interest are given in Tables IX and X, respectively.

Table of anisotropic thermal parameters, hydrogen coordinates, and listings of structure factor amplitudes for the three structures are available as supplementary material.

Acknowledgment. Financial support of this work by the CNRS is gratefully acknowledged.

Registry No. **1a**·PPN, 130352-16-8; **1c**·PPN, 130352-18-0; **2a**·PPN, 130352-20-4; **2b**·PPN, 130352-22-6; **2c**·PPN, 130352-24-8; **3a**, 130039-49-5; **3b**, 130352-25-9; **4a**, 130352-28-2; **4a**·$^1/_2CH_2Cl_2$, 138668-07-2; **4b**, 130377-83-2; **4b′**, 130352-26-0; $Ru_3(CO)_{12}$, 15243-33-1; PPN[$Ru_3(\mu\text{-}H)(CO)_{11}$], 71936-70-4; K[$S(C_5H_4N)$], 79236-86-5; PPN[$Ru_3(Cl)(CO)_{11}$], 110487-55-3; 2-hydroxypyridine, 142-08-5; 2-mercaptopyridine, 2637-34-5; 2-anilinopyridine, 6631-37-4; diphenylacetylene, 501-65-5.

Supplementary Material Available: Tables of anisotropic thermal parameters and hydrogen coordinates for the compounds PPN·**1c**, PPN·**2a**, and **4a** (6 pages); listings of observed and calculated structure factor amplitudes for the three structures (90 pages). Ordering information is given on any current masthead page.

(41) Enraf-Nonius. *Structure Determination Package*, 4th ed.; B. A. Frenz & Associates, Inc.: College Station, TX; Enraf-Nonius: Delft, The Netherlands, 1981.
(42) Coppens, P.; Leiserowitz, L.; Rabinovitch, D. *Acta Crystallogr.* **1965**, *18*, 1035–1038.
(43) Sheldrick, G. M. *SHELXS-86, Program for Crystal Structure Solution*; University of Göttingen: Göttingen, Federal Republic of Germany, 1986.
(44) Sheldrick, G. M. *SHELX-76, Program for Crystal Structure Determination*; University of Cambridge: Cambridge, England, 1976.
(45) Cromer, D. T.; Waber, J. T. *International Tables for X-ray Crystallography*; Kynoch Press: Birmingham, England, 1974; Vol. 4, Table 2.2B.
(46) Cromer, D. T.; Waber, J. T. *International Tables for X-ray Crystallography*; Kynoch Press: Birmingham, England, 1974; Vol. 4, Table 2.3.1.
(47) Stewart, R. F.; Davidson, E. R.; Simpson, W. T. *J. Chem. Phys.* **1965**, *42*, 3175–3187.